6-27-2022 1:30 PM

Three-dimensional Ultrasound Imaging for Characterization of Synovitis in First Carpometacarpal Osteoarthritis

Carla du Toit, *The University of Western Ontario*

Supervisor: Lalone, Emily, *The University of Western Ontario*

A thesis submitted in partial fulfillment of the requirements for the Master of Science degree in Kinesiology

Abstract

First carpometacarpal osteoarthritis (CMC1 OA) is one of the most common forms of OA and is a significant source of pain and disability for patients. Discrepancies between traditional imaging modalities and patient reported outcomes have led researchers to develop objective point of care-based imaging tools for assessing OA progression and treatment response. This thesis aims to describe the development and validation of a semi-submerged mechanical three-dimensional ultrasound device against the current clinical gold standard of magnetic resonance imaging (MRI). Additionally, this thesis will explore the relationship between the morphological presentation of synovitis, pain, physical function, and various semi-quantitative grading systems used in a CMC1 OA patient population.

Chapter 2 described the validation of the 3D US device which was conducted on a series of geometric and volumetric imaging phantoms, as well as a population of ten CMC1 OA patients. Images of the ten patients were acquired using a 3.0 Tesla MRI and our 3D US device. Two-raters manually segmented areas of synovial effusion and membrane hypertrophy during two separate sessions to evaluate intra- and inter-rater reliability. The results showed that 3D US had a strong concurrent validity with MRI and that it demonstrated excellent rater reliability. This indicates that 3D US shows great potential to provide clinicians with a quantitative method for monitoring synovitis in the small joints of the hand.

Chapter 3 presented in this thesis explored the implications of synovitis morphology presented in 3D US images and investigated synovial tissue volume as a possible predictor of CMC1 OA stage as determined by x-ray radiographic grading systems. Eaton-Littler (x-ray) and OMERACT (US) semi-quantitative grading systems were used to indicate OA and synovitis severity. These values were compared to the Australian Canadian Osteoarthritis Hand Index for

patient reported pain and disability, pinch grip force, synovial tissue volume, age and sex to determine which would be the most significant indicator patient reported pain.US images of CMC1 synovitis were analyzed and three distinct morphologies were identified based on location, volume and features of synovial effusion and hypertrophy. This study demonstrated that pinch grip was the most significant indicator of pain in CMC1 OA patients.

Keywords

Three-dimensional ultrasound, first carpometacarpal osteoarthritis, synovitis, osteoarthritis, two-dimensional ultrasound, MRI, validation, reliability, patient outcomes.

Summary for Lay Audience

The base of the thumb is a common site of osteoarthritis where patients typically experience symptoms of pain, stiffness, and weakness. An early indicator of thumb osteoarthritis is inflammation of the joint lining, called synovitis, which can be difficult to detect. Currently, x-ray images are the most common form of imaging used to view changes in the joints of patients with thumb osteoarthritis. X-rays are great for imaging bones; however, they are unable to show doctors information about the other joint structures that are affected by arthritis. These include your muscles, joint lining, and joint inflammation. Magnetic resonance imaging is an imaging method that is excellent for visualizing the soft tissue structures affected by osteoarthritis, however it is very expensive, has long waitlists, and is inaccessible to those individuals living in rural areas or cost-constrained healthcare systems. Additionally, neither MRI or x-rays can be used at a patient's bedside and patient positions for these scans can be uncomfortable maintain for long periods of time. In light of this, there is a serious unmet clinical need for inexpensive, rapid and safe imaging devices that can assess inflammation volumes at a patient's bedside. Very little information is available on how synovitis volume, shape and location relate to patient reported outcomes such as pain and functional disability. In this thesis, we describe our novel 3D US device for the hands and how well it performs when compared to more established imaging methods. Additionally, we use 3D US to assess the relationship between different OA imaging grading scales and pain in a group of patients with osteoarthritis at the base of their thumb. The results of these studies show that 3D US is able to provide accurate and precise measurements of inflammation when compared to MRI. We also showed that the relationship between pain and inflammation in thumb OA patients is not simple and that it may need to be considered within the context of which stage of disease a patient is presenting.

Co-Authorship Statement

This thesis integrates two original manuscripts. The first manuscript has been submitted for publication in the journal of Medical Physics and the second is in preparation for submission. As first author of each of these manuscripts, I have significantly contributed to all aspects of the work, including but not limited to, generation of research questions and study design, participant recruitment, data acquisition and analysis, manuscript drafting, and revisions. For the manuscript under review for publication, all co-authors have contributed to editorial feedback and have reviewed the manuscript prior to submission. The specific responsibilities and contributions of the co-authors have been outlined below.

Chapter 2 is an original research article entitled "Three-Dimensional Ultrasound to Investigate Synovitis in the Hand and Wrist" and is submitted for publication to the journal of Medical Physics. This manuscript was co-authored by Carla du Toit, Robert Dima, Sam Papernick , Melanie Jonnalagadda, Dr. David Tessier, Dr. Aaron Fenster and Dr. Emily Lalone. My specific contributions to the study included experimental design, participant recruitment, three-dimensional ultrasound (3D US) image acquisition, manual segmentation from magnetic resonance images (MRI) and 3D US images, phantom fabrication, device validation, data analysis and interpretation and manuscript preparation. Robert Dima was responsible for two-dimensional image acquisition, manual segmentation and image analysis. Sam Papernick contributed to study design and manual segmentation of imaging phantoms. Melanie Jonnalagadda was responsible for manual segmentation and data organization. Dr. David Tessier contributed to participant recruitment, administrative organization and ethics proceedings. Dr. Aaron Fenster provided supervision on image analysis, data analysis and interpretation as well as

manuscript writing. Dr. Emily Lalone was the Principal Investigator and provided supervision on study design, image analysis, data interpretation and manuscript writing.

Chapter 3 is in preparation for submission as an original research article entitled "Evaluation of Three-Dimensional Ultrasound as a Tool to Examine Synovitis Volume and Morphology in Relation to Patient Reported Outcomes**".** This manuscript was co-authored by Carla du Toit, Robert Dima, Dr. Tom Appleton, Dr. Nina Suh, Dr. Aaron Fenster and Dr. Emily Lalone. My specific contributions to this manuscript included experimental design, participant recruitment, three-dimensional ultrasound (3D US) image acquisition, manual segmentation from 3D US images, data analysis and interpretation and manuscript preparation. Robert Dima was responsible for two-dimensional image acquisition, manual segmentation and image analysis. Dr. Tom Appleton provided clinical insight and guidance on image analysis and result interpretation. Dr. Nina Suh contributed to patient recruitment and x-ray scoring. Dr. Aaron Fenster contributed to experimental design and manuscript revision. Dr. Emily Lalone was the Principal Investigator for this study and provided supervision on experimental design, image analysis, data interpretation and manuscript revision.

Acknowledgements

This work would not have been possible if it were not for the support of my supervisor, advisors, volunteers, family, and friends. These individuals have guided me through the past two years and have made this experience invaluable to me.

First and foremost, I would like to thank my supervisor, Dr. Emily Lalone. Emily, thank you for the freedom, unconditional support, and mentorship you have given me to achieve my goals throughout the last two years and to become the person I am today. You are truly an inspiration to all young researchers, and I will forever be grateful for the guidance and amazing learning experience you have given me.

Thank you to my primary collaborator Dr. Aaron Fenster. Aaron, thank you for the incomparable excitement and leadership you have given me during my time on your team. Your enthusiasm for learning and unwavering support has provide me with an unrivalled learning experience that I will strive to foster wherever I go in my future endeavours. I will always treasure your many stories and lessons that have brightened many of my more challenging days.

Thank you to my advisory committee, Dr. Tom Appleton and Dr. Nina Suh. I will always remember your encouragement and commitment to helping me complete this project. Thank you to all the volunteers and patients who have made this research project possible. Without you we would not have been able to achieve our goals in striving towards more efficient and better healthcare.

Thank you to all the past and present members of the Lalone and Fenster labs and the many other individuals at Robarts who have made my graduate experience exciting and enjoyable. I would like to thank David Tessier for all his help during every step of my research project. David, you truly deserve your nickname, the “Wolf”. I truly believe there is not a

problem that you cannot fix if you put your mind to it! Thank you for always being so kind and willing to help solve any problems we may face in the lab. Thank you to Claire Park for your friendship, support, and kindness Thank you to Nathan Orlando for your compassion, excitement, and motivation. It has been an amazing experience working with you and I look forward to seeing all your future achievements. Thank you, Melanie Jonnalagadda, for all you dedication and kindness. Thank you, Sam Papernick for your friendship, mentorship and motivation. Our weekly runs in Gibbons Park will greatly be missed. Thank you to Robert Dima for your friendship, mentorship, and expertise. My project would not have been possible without you on the team, and I look forward to many more deep conversations and future endeavours. I would be remiss if I did not thank the numerous other people who have supported and helped me throughout my graduate degree, including but not limited to Elizabeth Norman, Lauren Stratman, Kevin Barker, Lori Gardi, Jeffrey Bax, Igor Gyacskov, Jacques Montreuil, and Chandima Edirisinghe.

Thank you to my friends who have supported me and have brought fulfillment to my life over the past few years. Tiana Trumpour, thank you for your unwavering support through the ups and downs of graduate school. You have helped me through the good and the challenging times and I am honoured to call you my friend. Olivia and Nicole, there is never a dull moment in your presence, and I would not want my life any other way. Liv, from the moment I stepped foot on to campus for the first time to the last time I left the gates you have been there for me and I will always be grateful for your friendship.

Thank you to my family for the love and support you have always given me. Ma en Pa, dankie dat julle altyd by my staan en vir al die opofferings wat julle vir my maak. Ouma en Oupa, dankie vir julle onwrikbare ondersteuning en aanmoediging. Tannie Sharon en Oom

Willem, dankie vir julle entoesiasme en ondersteuning. Dit beteken die wêreld vir my. Ek sal altyd daarna streef om julle trots te maak. Thank you to my sister, Nicola for her support and encouragement.

Anton, thank you for your unconditional love and support through all these years. Thank you for always embracing my goals, encouraging me to achieve them, and for making sure I have all the tools I need to succeed. You bring light and laugher into my life, and I am incredibly grateful and lucky to have you as my partner.

Thank you to my examiners, Dr. Derek Pamukoff, Dr. Trevor Birmingham, and Dr. Joy McDermid. Thank you for the time and effort you have dedicated to my education by examining my thesis and participating in my defense.

Finally, I would like to acknowledge the following sources of funding for supporting this work: the Canadian Institutes of Health Research, the Western Bone and Joint Institute and the Western Strategic Research Fund.

Table of Contents

List of Tables

List of Figures

List of Appendices

List of Abbreviations

2D	Two-dimensional
3D	Three-dimensional
AUSCAN	Australian Canadian Osteoarthritis Hand Index
CMC	Carpometacarpal
CMC1 OA	First Carpometacarpal Osteoarthritis
DSC	Dice Similarity Coefficient
EL	Eaton- Littler Grading System
FSE	Fast Spin Echo
FS	Fat Saturation
HD	Hausdorff Distance
ICC	Intraclass Correlation Coeffient
KOA	Knee Osteoarthritis
MRI	Magnetic Resonance Imaging
OA	Osteoarthritis
OARSI	Osteoarthritis Research Society International
OMERACT	Outcome Measures in Rheumatoid Arthritis Clinical Trials
PD	Photon Dense
SD	Standard Deviation
STV	Synovial Tissue Volume
US	Ultrasound

Chapter 1

1 Introduction

Over the last century, medical imaging has experienced dramatic advancements since the discovery of x-rays in 1895. Today, medical professionals and researchers can view the body in fantastic detail with the use of various imaging modalities such as x-ray radiography, ultrasound (US), computed tomography (CT), positron emission tomography (PET), and magnetic resonance imaging (MRI). The field of medical imaging has had a significant impact on medical diagnostic, monitoring, and treatment methods. However, the human body is comprised of extremely complex anatomy and physiological systems, which often cause challenges in acquiring images. As our knowledge of imaging technology increases, new imaging devices and methods are being developed to help overcome the limitations associated with visualizing the body and its various pathologies. However, with increased development and use of medical imaging, concern over radiation exposure, patient accessibility, high associated operating costs and resulting cascades of care have significantly intensified[1].

Imaging of musculoskeletal pathology for diagnostic and monitoring purposes are currently acquired using x-ray radiography, MRI, and US. These methods are associated with limitations in contrast, accuracy, and sensitivity when assessing whole joint pathology such as arthritis, due to the multifactorial nature of these diseases[2]. Osteoarthritis (OA) has soft tissue, bone, and metabolic characteristics that are difficult to image using only one of the of imaging modalities previously mentioned. Three-dimensional (3D) ultrasound imaging is a relatively new imaging modality within the field of musculoskeletal imaging, which can provide a method for overcoming some of the limitations associated with x-rays, MRI, and two-dimensional (2D) ultrasound. 3D US has previously been validated for use in healthy knee patients, gynecological,

vascular, neonatal, liver, and prostate oncology applications[3–5]. However, 3DUS has not been validated for monitoring osteoarthritis in the more complex joints of the hand and thumb, where small anatomical structures and physiological changes mean significant changes in joint health and disease progression.

This thesis will explore the application of a submerged mechanical 3D US device as a point of care imaging modality to provide clinicians with a method for monitoring osteoarthritis disease progression and treatment response. Specifically, this thesis will investigate the application of this 3D US device for monitoring synovial volume as an indicator of osteoarthritis pathogenesis in the first carpometacarpal (CMC1) joint of the thumb. Validation of this imaging method may potentially impact workflow for primary care, rheumatology, orthopedic, and sports medicine clinics by providing a method for acquiring 3D images at the patient's bedside. The remainder of this chapter provides background information on CMC1 OA diagnosis, treatment, and monitoring, as well as principles of 3D US and other medical imaging modalities. It will also describe the underlying unmet clinical needs, hypothesis, and objectives of this thesis.

1.1 First Carpometacarpal Osteoarthritis

Osteoarthritis is the second most common chronic disease in the world and the most prevalent form of arthritis[6]. Traditionally OA was considered a disease of the articular cartilage and bone. However, with recent advances in medical imaging technology, we now understand that OA is a whole joint disease. The definition of OA has been updated to describe it as a disease that influences the articular cartilage, subchondral bone, vascular structures, and synovial membrane function[7]. OA can affect any joint in the body but those most commonly affected include the knees, hips, proximal interphalangeal joint, and the carpometacarpal joint of the

thumb. OA patients typically experience pain, functional disability, and decreased overall quality of life. Additionally, studies have reported high comorbidity with cardiovascular disease, diabetes, anxiety, and depression[8–10].

Knee osteoarthritis has been studied extensively over the past few decades due to its high prevalence and associated disability however, investigation into OA of smaller non-weight bearing joints still requires exploration. With the increase in the average age of the world's population, we are experiencing a rise in the prevalence of OA. The prevalence of CMC1 OA has been reported to be as high as 33% in some study populations (the Rotterdam Study) and is higher in post-menopausal women[11,12]. As such, it is imperative for studies to examine avenues for earlier detection and treatment of OA.

1.1.1 Hand and First Carpometacarpal Joint Anatomy

The human hand is comprised of 3 sections, the wrist, palm, and fingers which include 27 bones. The osseous anatomy of the hands consists of the distal heads of the radius and ulna, eight carpal bones, five metacarpal bones, five proximal phalangeal, five middle phalangeal, and five distal phalangeal bones (Fig. 1.1.1.1.1).

Articulations between the radius, ulna, carpal, and metacarpal bones constitute the wrist joint. The proximal row of carpal bones consisting of the scaphoid, lunate, triquetrum, and pisiform articulate with the distal ends of the radius and ulna. The distal row of carpal bones (trapezium, trapezoid, capitate, and hamate) articulate with the five metacarpal bones to form the palm of the hand. Each of the five metacarpal bones connects to a phalange via the metacarpophalangeal joint. Each finger in the hand is made up of 3 phalanges except for the thumb, which is only comprised of 2. It is the complexity and the large number of bone articulations that allow for a wide range of movements in the hands[13].

1.1.1.1 First Carpometacarpal Joint

The 1st carpometacarpal joint is a biconcave-convex saddle synovial joint that is responsible for all thumb movements. The joint contains the proximal first metacarpal, trapezium, hyaline cartilage, ligaments, muscles, and a synovial membrane. Thumb motion is controlled by extrinsic flexors, extensors, abductors, and intrinsic muscles. Extensor pollicis brevis and abductor pollicis longus are the two main muscles that move the CMC joint through extension and abduction motions. Extensor pollicis brevis inserts on the proximal phalanx and runs along the radial aspect of the anatomic snuff box, while abductor pollicis longus inserts at the base of the first metacarpal. The intrinsic muscles of the thumb consist of adductor pollicis and the thenar muscles on the ventral side of the hand. The thenar group of muscles consists of abductor pollicis brevis, flexor pollicis brevis, and opponens pollicis. These muscles are responsible for flexion, abduction, and opposition of the thumb. Adductor pollicis inserts at the base of the proximal phalanx and is responsible for adduction and opposition[14].

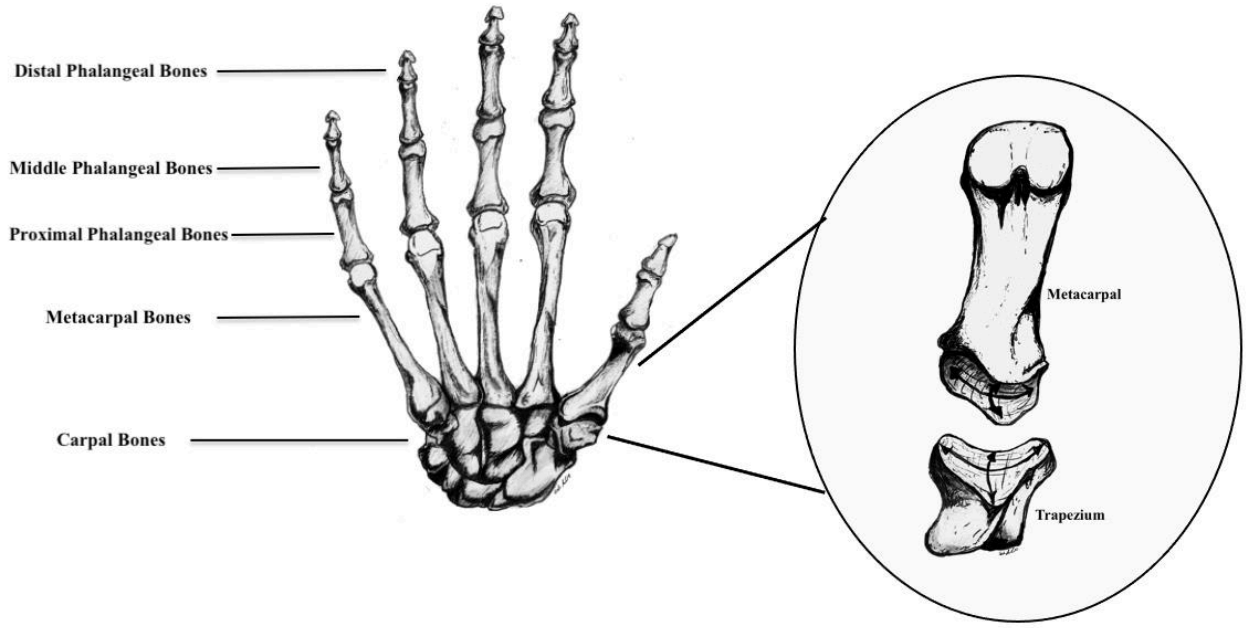

Figure 1.1.1.1.1: **Anatomical diagram depicting the hand osseous anatomy.** This figure includes the distal, middle, and proximal phalangeal bones, metacarpals, and carpal bones. Emphasis is added to the metacarpal and trapezium carpal bone which make up the first carpometacarpal joint of the thumb.

1.1.1.2 The Synovium

The synovium is the soft tissue lining of diarthrodial joints, tendons, and bursae containing hyaluronic acid, referred to as synovial fluid. The synovial membrane has two layers of cells, the first is the intima, and the second is the underlying tissue, called the subintima. The intima is mainly composed of macrophages and fibroblasts, cells that function as immune defense and maintain the structural framework, respectively. The subintima contains blood and lymphatic vessels, fibroblast, and other infiltrating cells which are contained in a collagenous extracellular matrix[15]. Typically, the normal synovial membrane is only about 25-45mm thick cross-sectionally.

However, in patients with rheumatoid and osteoarthritis, this thickness increases dramatically due to increases in macrophages[16]. This infiltration is reported to be associated with stromal edema and proliferation of the blood vessels.

1.1.2 Risk Factors

Risk factors for osteoarthritis can be separated into three major categories, including systemic, local joint, and extrinsic factors that act on joints[17]. Figure 1.2 highlights these risk factors and how they can interact. Systemic risk factors increase the overall susceptibility of the individual to joint pathology and local joint biomechanical factors that have a significant impact on the optimal functioning of a joint. Factors categorized into the systemic group include age, gender, ethnicity, generics, bone density, nutritional factors, and inflammation. Age and female sex are the most well-known risk factors for CMC1 OA[11,18]. Female sex has been an undisputed risk factor for CMC1 OA as it amplifies the age-related increase in risk for OA in the hands, knees, and multiple joints. Many studies have consistently demonstrated that females have a higher prevalence of CMC1 OA than males, according to biological sex[11,12,19]. The prevalence of OA also increases in certain racial and ethnic groups. OA is more prevalent in Western societies such as Europe and North America, and targets African-American women more than Caucasian or Asian women[20].

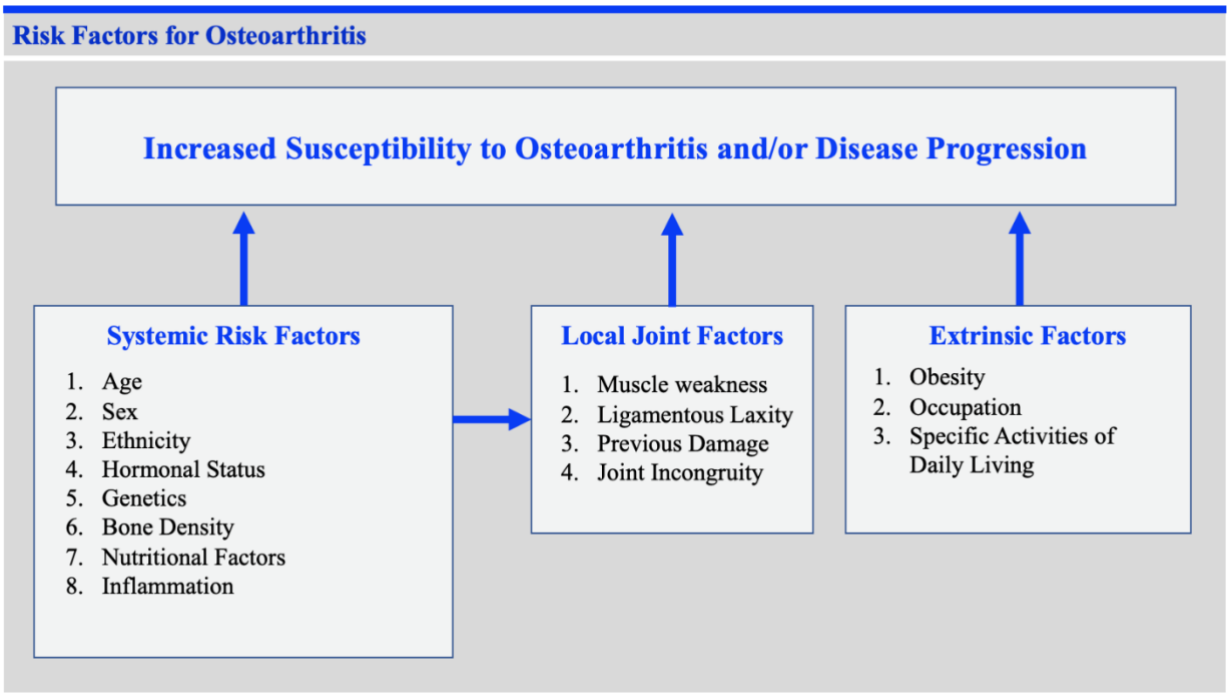

Figure 1.1.2.1: Risk factors of OA. Diagram depicting the different types of OA risk factors and how they interact to put individuals at risk for developing OA**.**

1.1.3 Clinical Presentation and Symptoms

CMC1 OA is diagnosed clinically by a physician to evaluate the severity of patient symptoms. Symptoms include localized pain, inflammation, instability, weakness, and loss of pinch grip strength. As OA progresses to more severe stages of pathology, the CMC1 joint becomes stiff and forced into adduction, resulting in joint subluxation, first metacarpophalangeal joint hyperextension, and proximal migration of the first metacarpal [21,22]. The primary goals of treatment interventions are to prevent further disease progression and to alleviate symptoms. Clinical examinations of CMC1 OA are typically supplemented with medical imaging to determine disease severity and treatment progression[7]. Traditionally, standard posterior-anterior, lateral, and oblique views are acquired using plain x-ray radiographs. These views may also be supplemented with CMC1 joint stress views, which are acquired by asking the patient to press their thumbs together. This view allows for increased visualization of the joint articulations and

makes assessment of joint subluxation easier[23–25]. Medical imaging is helpful to evaluate disease severity or monitoring progression however, it is rarely required to confirm the diagnosis of CMC1 OA[26]. Semi-quantitative grading systems, such as the Eaton-Littler (EL) grading system, have provided set guidelines for defining the presence of CMC1 OA. Osteophyte presence and size, degree of joint subluxation, and severity of sclerosis are all characteristics that indicate disease severity. The EL grading scale defines OA severity in four grades (1-4, Subtle CMC1 joint space widening to arthritic changes in the CMC1 joint with scaphotrapezial arthritis)[27].

1.1.4 Disease Progression and Treatment Options

OA is not traditionally considered an inflammatory arthropathy. This is due to the relative lack of neutrophils found in the synovial fluid of OA patients and the lack of systemic manifestations of inflammation seen in comparison to rheumatoid arthritis. Despite this, OA symptoms regularly include swelling, stiffness, and pain in the affected joint, suggesting an inflammatory response[28]. It is now recognized that inflammation has an important role in OA pathogenesis and disease progression. Several studies have demonstrated that there are several key changes present in the synovium of patients with OA knees[29,30]. These changes included thickening of the synovial lining layer, increased vascularity, and inflammatory cell infiltration[31]. Although these changes are more pronounced in more advanced stages of OA, they are present from the earliest stages of the OA disease process. The classical OA spectrum ranges from significant synovial effusion and hyperplasia of the lining layer, including cellular infiltrate composed of lymphocytes and monocytes, through to a synovial membrane that has thickened due to fibrosis of the tissues involved[29,32]. Benito et al. reported that early knee OA patients have higher levels of macrophage infiltration and more blood vessel proliferation markers than those individuals who have advanced OA[31]. They also demonstrated that early knee OA patients

expressed higher levels of inflammatory mediators such as interleukin-1 and tumor necrosis factor-alpha than those at later stages of OA. These pro-inflammatory cytokines have been proven to be involved in the initiation and progression of articular cartilage degeneration in OA[33].

There is currently still no cure of OA however, several treatment methods focus on alleviation of patient symptoms. Expert organizations such as Osteoarthritis Research Society International (OARSI), the European League Against Rheumatism (EULAR), and the American College of Rheumatology have published several guidelines for managing OA at various joints, including the hands, hips, and knees[34–39]. For symptomatic CMC1 OA patients, treatment guidelines recommend combining hand therapy and orthosis with pharmaceutical interventions. Although the CMC1 joint is not a weight-bearing joint, physical activity can improve overall health, and joint-specific exercises can increase the strength and flexibility of the muscles that act as the dynamic stabilizers of the thumb. The combination of these physical therapy interventions has demonstrated considerable variation in patient outcomes where some patients report substantial improvement in pain relief and physical function whereas others experience no improvement[40].

Pharmaceutical therapies are commonly included in the treatment plans of OA patients. Clinicians commonly prescribe medications such as paracetamol, non-steroidal anti-inflammatory drugs, and corticosteroids. Paracetamol is commonly prescribed due to its cost-effectiveness and safety. However, systematic reviews have shown either conflicting results or low efficacy for its use in pain management for OA[41]. A meta-analysis by Zhang et al. directly comparing paracetamol and NSAIDS, demonstrated that NSAIDS provided better pain relief. However, it is important to note that there is high variability in patient responses to these drugs[42].

When more conservative treatments for CMC1 OA fail to relieve patient symptoms, intra-articular injections such as corticosteroids and hyaluronic acid can be the next step in treatment options[43,44]. These intra-articular injections aim to relieve pain and reduce inflammation however, effectiveness is not well reported and the available literature on the topic has significant limitations[45,46].

Early surgical interventions for CMC1 OA include ligament reconstruction with or without tendon interposition. Later surgical interventions include arthroplasty, where all or part of the damaged thumb joint is removed and replaces with an artificial implant. Arthrodesis, fusion of the bones, is done to fuse the first metacarpal and the trapezium. This procedure has a high complication rate and causes loss of mobility in the CMC joint, including the ability to lay the palm flat and put the fingers and thumb into a cone shape.

1.2 First Carpometacarpal Osteoarthritis Imaging

1.2.1 X-ray Radiography

X-ray radiography is currently the most commonly used imaging modality in the assessment of OA. This is due to the cost-effectiveness and availability associated with this modality. In 1973 Eaton and Littler first described a four-stage radiographic grading system, which was then adopted as the standard method for assessing radiographic evidence of CMC1 OA[47]. In 1987, the scale was upgraded to include scaphotrapezial arthritis in the fourth stage. Radiography is widely accessible, has short acquisition times, and is associated with less discomfort than what is reported with other imaging modalities such as MRI. Joint space narrowing, sclerosis, subchondral cysts, and osteophytes are all imaging features associated with OA disease and progression (Fig.1.3). Radiography has several limitations to consider when using it as an imaging modality for osteoarthritis. Most prominently, the lack of soft-tissue

contrast associated with radiography excludes essential information about the cartilage, synovium, and other structures surrounding the CMC1 joint. Similar to what has been reported in the knee OA literature, changes in the position of the thumb in radiographic images can change critical values such as joint space width and the number of osteophytes observed[48,49]. Additionally, the features of interest in these radiographic grading systems are typically indicative of more advanced stages of OA, potentially leading to a delay in appropriate treatment.

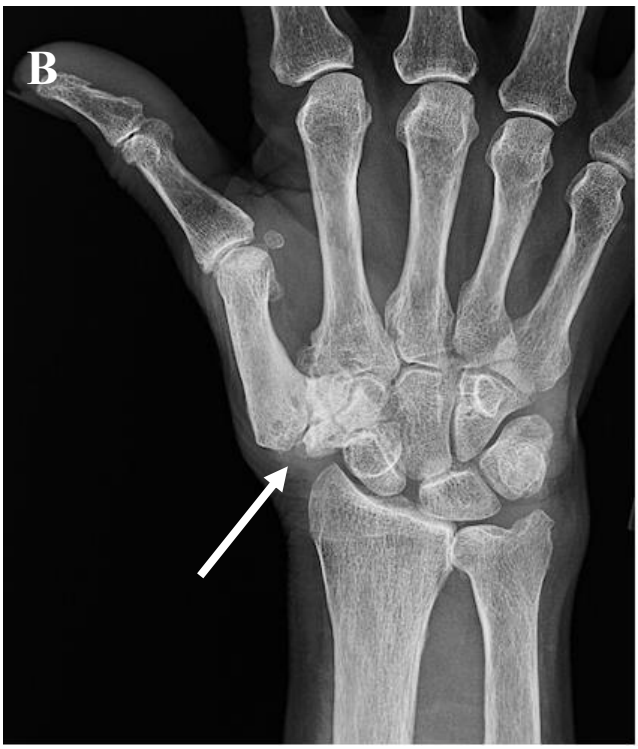

Figure 1.2.1.1: Radiograph of a patient with Eaton- Littler stage 4 CMC1 OA . This image shows a decrease in carpometacarpal joint space, subchordal sclerosis, subluxation of the CMC1 joint and arthritic involvement of the scaphotrapezial joint.

1.2.2 Magnetic Resonance Imaging

Magnetic resonance imaging is an imaging modality that is excellent for overcoming the limitations associated with radiography. MRI provides excellent soft tissue-contrast, enabling better assessments for joint structures such as articular cartilage and the synovium. When examining the CMC1 joint clinicians are able to visualize the synovium, anterior oblique ligament, posterior oblique ligament, radial collateral ligament, and the surround muscles (abductor pollicis longus, extensor carpi radialis longus). The health and integrity of these structures play a very important role in joint stabilization and are the targets for early manifestations of OA. MRI is the current reference standard for imaging OA due its high spatial resolution, three-dimensional (3D) imaging capabilities and excellent soft tissue contrast[50]. The 3D nature of MRI also allows for quantitative measurements of key OA factors such as synovial tissue volume. These measurements can be applied to disease monitoring protocols and can be used to assess treatment effectiveness. The OMERACT Hand and Osteoarthritis Magnetic Resonance Scoring System (HOAMRIS) is an example of a semi-quantitative measurement tool specifically for use in MR imaging of the hand[51].

Despite the advantage of excellent soft-tissue contrast associated with MRI for monitoring CMC1 OA, it is also associated with many limitations. MRI is associated with long waiting lists, high manufacturing, and operating costs, which includes the requirement of installing specialized MRI facilities and the machines themselves. These added costs make MRI largely inaccessible in cost constrained healthcare systems and in rural communities resulting in patients having to travel and only increases to cost-burden on those most vulnerable. The limited amount of MRI facilities available across the world results in longer waitlists and potentially further delays treatment planning. A study conducted by Ogbole et al. highlighted the extent of

this inaccessibility in 16 Western African countries as found that there were only eighty-four MRI units to serve a combined population of 372,551,411 people. Additionally, these units were not equally spread across these countries, with Nigeria accounting for 58% of the available units[52]. In addition to these limitations, acquiring MR images of the CMC1 joint is a long and uncomfortable experience for most patients. Patients are asked to lay prone in the core with their hand extended above their head. They are also required to stay still for the duration of the scan, which usually takes about thirty minutes. When we take into consideration who our patient population is, we can see that these patients typically have other common musculoskeletal impairments, such as shoulder impingement, that makes staying still in the required position very uncomfortable.

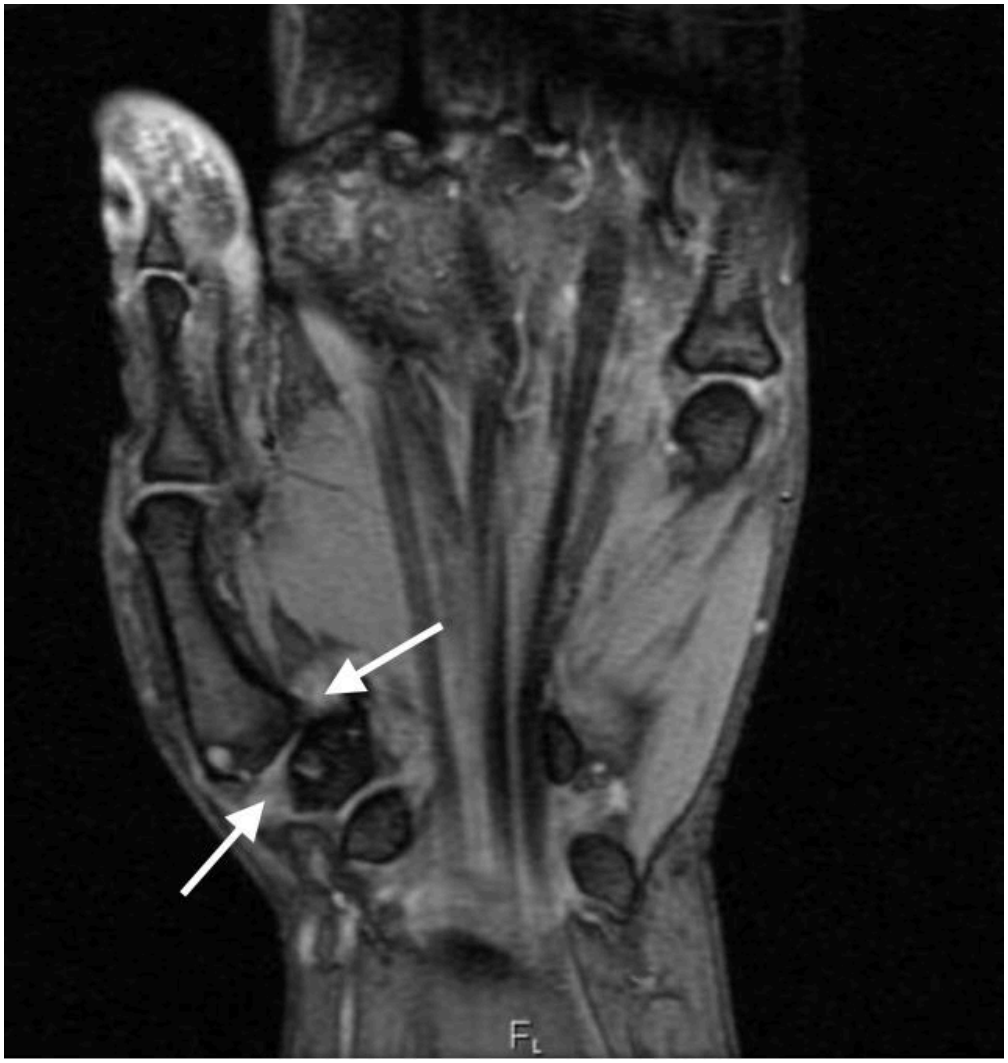

Figure 1.2.2.1: MRI of a CMC1 patient. This figure includes arrows highlighting the joint.

1.2.3 Conventional Ultrasound

Two-dimensional (2D) US imaging is a widely accessible imaging modality that uses high-frequency acoustic sound waves transmitted through a water-based coupling agent and received by a transducer. Ultrasound images are acquired in real-time, meaning that the images are continually acquired as the transducer is manipulated across the area of interest. This allows

operators to assess the movement kinetics of internal structures such as ligaments, muscles, and tendons. Ultrasound can also be used to assess fluid movement using applications such as Doppler imaging. The transducers can be manipulated into several different views and orientations to acquire images that would typically be unattainable using radiography. Synovial effusion appears hypoechoic on US images while synovial membrane hypertrophy is slightly less hypoechoic. This is due to the difference in water content in the structures and is regularly used to determine progression of OA in clinics. 2D US has increasingly been integrated into orthopedic and rheumatology clinics due to its portable point of care nature and its image resolution. US is very accessible to all patients as images can be acquired at bedside with very minimal discomfort for the patient. This overcomes some of the limitations associated with MRI and patient physical accessibility and discomfort. Multiple studies have examined the use of 2D US for osteoarthritis monitoring with focus on articular cartilage thickness, synovitis, cysts, and abnormal osteochondral growths[53,54,55,56]. In 2016, the European League Against Rheumatisms (EULAR) and the Outcomes Measures in Rheumatology (OMERACT) US Working Group developed a semi-quantitative US scoring system for hand OA[57].

2D US has several significant limitations. The first limitation is that 2D US acquires 2D images of inherently 3D anatomy. Traditionally, during a conventional ultrasound examination, the operator is required to mentally transform a series of 2D images into a subjective impression of the 3D anatomy. Thus, the accuracy and precision of measurements and discissions made for treatment are heavily reliant on operator skill and expertise. Diagnosis, treatment, and monitoring of osteoarthritis often requires accurate estimation of cartilage thickness and synovial tissue volume. With conventional US, volume calculation utilizes simple measurements such as height, width, and length in only two orthogonal views. Usually, the operator also must assume

idealized shape which is very rarely the case when investigating synovial effusion and membrane tissue volume in the CMC1 joint. This practice is both inaccurate, highly operator dependent and has high variability. Additionally, 2D US imaging may not be appropriate for acquiring volumetric data for longitudinal studies, due to the challenges associated with standardizing patient and transducer position during consecutive scanning sessions[58]. Finally, the field of view in 2D US is limited to the length of the transducer, meaning that it is challenging to examine the entire joint and tissues of interest with one 2D image. Therefore, multiple images are often required, resulting in increased scanning session times, increased difficulty in interpretation with changes in the surrounding anatomy.

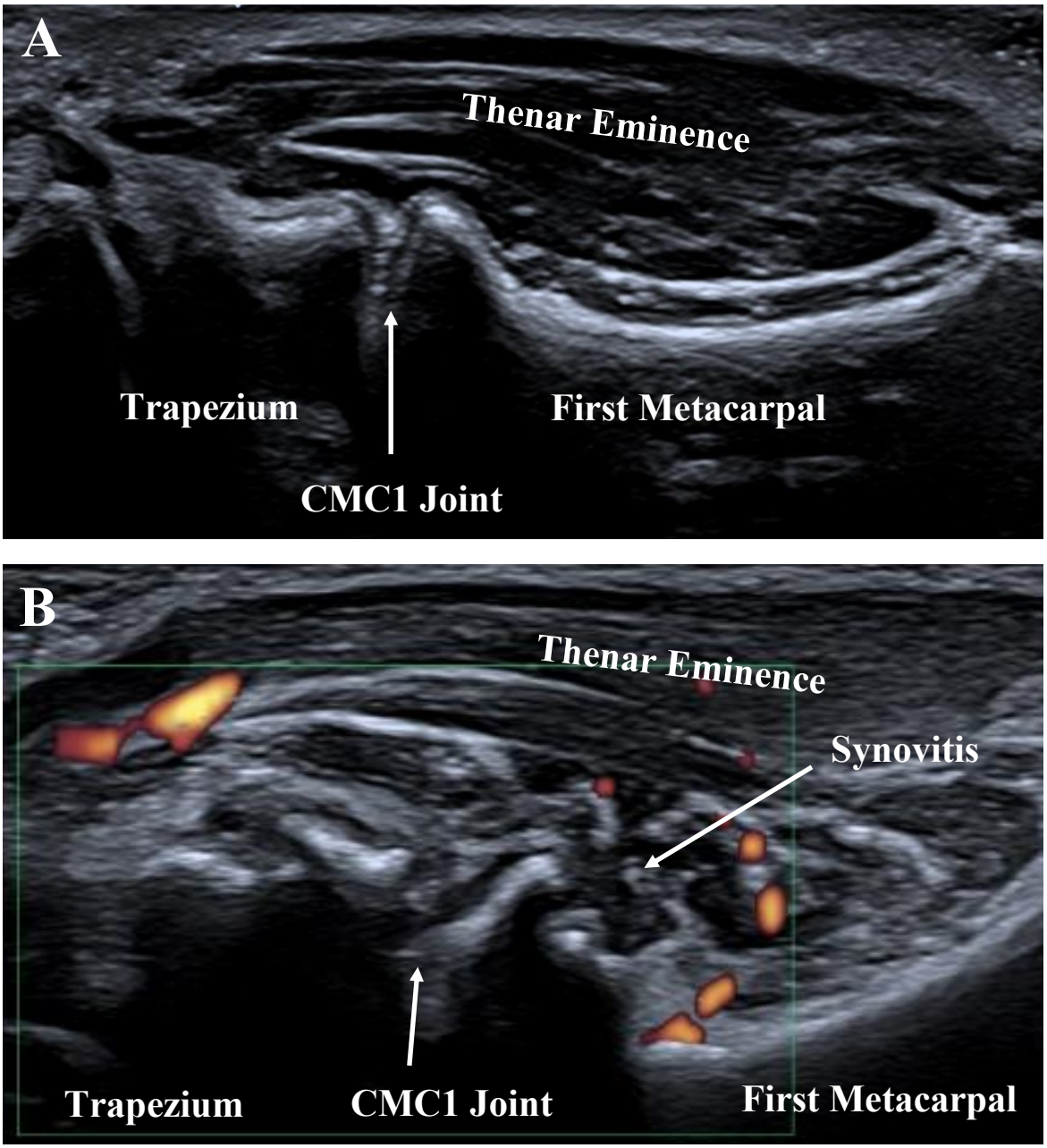

Figure 1.2.1 :2D US images of the CMC1 joint. This figure shows a healthy volunteer (A) and in a patient with OA (B). Images were acquired with an Aplio i800 US machine (Canon Medical Systems Corporation, Otawara, Tochigi, Japan). This system was equipped with a 14L5 linear transducer with an operating frequency of 10 MHz.

1.3 3D Ultrasound Imaging

3D US imaging has the potential to overcome many of the limitations associated with conventional US imaging. 3D US imaging follows the same physical principles as 2D US in that acoustic wave are produced and received by piezoelectric crystals within the ultrasound transducer. The most significant difference between 2D and 3D US imaging is that 3D US provides the operator with an interactive 3D reconstruction of the anatomy, effectively removing the need for mental transformation of the images[58].

Currently, there are three different methods for acquiring 3D US images. These include free hand, 2D array transducers and mechanical transfer. The first method, free-hand scanning requires the operator to manually move a 2D transducer across the area of interest while the position and movement of the transducer is recorded by an optical tracking system. In order to optimally track the position of the transducer, a minimum of three markers are required to cover all degrees of freedom. The tracking system uses infrared cameras to track these passive markers. This method is similar to other methods used to track motion and limb movement in biomechanical studies. The second approach requires a specialized US transducer that contains a matrix of 2D array elements. The matrix elements allow the transducer to acquire images in two different planes simultaneously, however the increased amount of required elements increases the manufacturing cost of these transducers[59,60]. Additionally, a complicated file transferring processes is required to export these images from the US machine, which is required for any post-acquisition processing needed. The third acquisition method uses a motorized drive mechanism to translate, tilt or rotate the 2D US transducer across the area of interest while an encoder and computer records the position. As the transducer is translated, hundreds of 2D US images are acquired and the exact orientation and position of each image is known because the speed, distance and frame rate of each image is known[61]. The 2D US images are then added

together using software to create the 3D reconstruction, similar to adding together slices of bread to form a loaf[58].

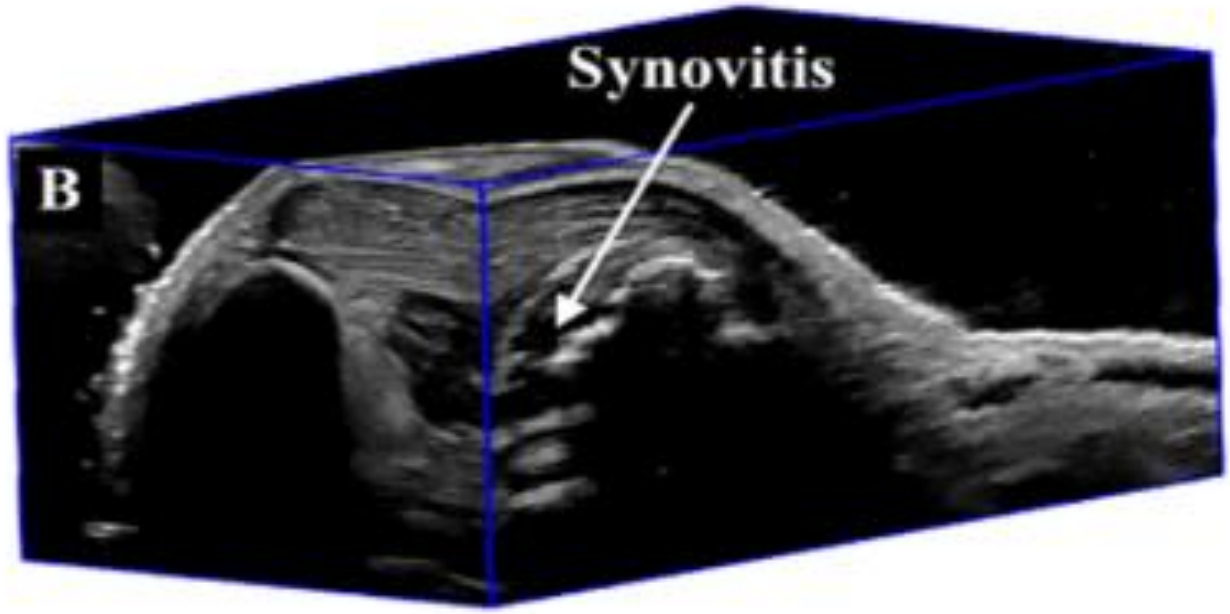

Figure 1.3.1: **3D US image of a CMC1 OA joint**. This figure shows the CMC1 joint of a patient with OA indicating the anechoic section of synovial effusion and labeled acquisition and reconstruction planes.

In this thesis, we have chosen to use a linear mechanical acquisition method as images are acquired at set spatial intervals that produce a rectangular geometry after acquisition (Fig. 1.6). As we are focusing on the small CMC1 joint of the thumb, the field of view of the transducer is not a significant concern for this project. However, expansion of this imaging method to other, larger joints would benefit from the increased field of view as shallower depths associated with the linear scanning approach.

Once a 3D US image is formed, it contains multiple image planes. The orientation in which the original 2D US images were acquired is referred to as the acquisition plane and is the plane with the highest spatial resolution (Fig.1.6). This plane has the same spatial resolution as the 2D US transducer. The plane perpendicular to the acquisition plane is referred to as the reconstruction plane (Fig.1.6). The spatial resolution for the reconstruction plane is equal to that of the elevational resolution of the transducer. Spatial resolution is directly dependent on the depth setting and the frequency of the 2D US machine. When acquiring 3D US images, the translational speed of the transducer needs to be matched to the sampling rate of the US machine. Changes made to the scan distance or translation speed will affect the 3D US acquisition time. A typical 3D US scan takes approximately less than 20 seconds. These fast acquisition times, in addition to the customizability of the transducer holders and the decrease in operator dependency makes 3D US scanning an attractive method for quantitatively measuring synovial tissue volumes. This application could potentially be critical for the diagnosis and monitoring protocols for CMC1 OA.

1.4 Current Challenges of Image-Based CMC1 OA Monitoring

1.4.1 Unmet Clinical Need and Previous Work Completed

There is an unmet clinical need for point-of-care imaging devices that can provide quantitative methods for characterizing and monitoring synovitis in the CMC1 joint. We believe that 3D US may provide a potential method to satisfy this need. However, the development of new imaging devices requires rigorous testing to determine validity, reliability, and feasibility before implementation can be considered. Therefore, evaluation of current and possible new clinical workflow is essential when considering the design and adoption protocols for new

imaging devices. Studies previously conducted in our lab have evaluated the accuracy and precision of the mechanical linear translation method using geometric imaging phantoms and in the knees of healthy volunteers[62,63]. These studies have shown that the linear scanning technique can produce volumetric measurements with less than 2% error compared to known phantom dimensions. Therefore, studies examining the measurement capabilities and clinical feasibility of using 3D US imaging are needed for the small joints of the hand. Additionally, more work is needed to understand the pathogenesis of synovitis in the context of CMC1 OA, how it presents morphologically in US and how this is related to patient-reported outcomes.

1.4.2 Hypothesis

The overall objective of this thesis is to advance the use of MSK 3DUS and identify sonographic features associated with osteoarthritis. As an initial clinical application, this thesis examines synovitis and inflammatory features associated with CMC1OA (base of the thumb osteoarthritis).

1.4.3 Objectives

There are three primary objectives for this work:

1. To assess the linear and volumetric measurements capabilities of the proposed 3D US machine using imaging phantoms (Chapter 2).
2. To validate and measure the precision of 3DUS-based measures of synovial tissue volume using gold standard MRI-based measurements in CM1 OA (Chapter 2).
3. To evaluate the intra- and inter-rater reliability of our manual synovial tissue volume measurements.

4. To examine sonographic features associated with CMC1 OA in a cohort of patients. Sonographic features include synovial tissue volume and effusion morphology (Chapter 3).
5. To determine if synovial tissue volume is a predictor of patient-reported arthritic pain (Chapter 3).

In response to the above objectives, the hypotheses for this work are:

1. Linear and volumetric measurements capabilities will be less than 2% ground truth.
2. 3DUS will be valid (within 5%) and reliable for measuring synovial tissue volume.
3. 3DUS-based measure of synovial tissue volume will be reliable within and between raters.
4. 3DUS will be a valuable tool to visualize sonographic features associated with CMC1 OA while providing sufficient image resolution and distinct morphological features of effusion (margin and geometry) vs. hypertrophy that will be useful to categorize phenotypes that may be associated with stages of early to advanced CMC1 OA.
5. Synovial tissue volume will be a significant predictor of patient-reported arthritis pain.

1.5 Thesis Outline

This thesis will address the objectives previously stated in two manuscripts (Chapter 2 and Chapter 3).

Chapter 2: Three-Dimensional Ultrasound to Investigate Synovitis in the Hand and Wrist

Chapter 2 describes the development and validation of a semi-submerged mechanical 3D US device that is intended for monitoring synovitis and the progression of CMC1 OA. The application of this point-of-care system to the small joints of the hand will improve clinical

workflow and potentially provide clinicians with more effective methods for quantitatively monitoring the effect of synovitis on CMC1 OA progression. In addition, this device could be beneficial in research settings by providing a tool for assessing OA longitudinally and monitoring intervention response.

Chapter 3: Evaluation of Three-Dimensional Ultrasound as a Tool to Examine Synovitis Volume and Morphology in Relation to Patient-Reported Outcomes

Chapter 3 describes the application of 3D US to a CMC1 patient population to evaluate how synovial tissue volumes could relate to patient-reported pain and disability scores on the AUSCAN. Additionally, we describe the various synovitis morphological features observed in US in our study population and examine how these differences could influence how the relationship between ratings on the AUSCAN relate to synovial tissue volume and other image-based methods OA staging.

Chapter 4: Conclusions and Future Directions

This chapter provides an overview of the previous two chapters and aims to discuss the limitations and future directions required to further our understanding of 3D US as a tool for monitoring OA in non-weight-bearing joints.

1.6 References

1. Zanzonico PB. Benefits and Risks in Medical Imaging. *Health Physics*. 2019;116(2):135-137. doi:10.1097/HP.0000000000001038

2. Evangelisto A, Wakefield R, Emery P. Imaging in early arthritis. *Best Practice & Research Clinical Rheumatology*. 2004;18(6):927-943. doi:10.1016/j.berh.2004.07.002

3. Clendenen SR, Robards CB, Clendenen NJ, Freidenstein JE, Greengrass RA. Real-Time 3-Dimensional Ultrasound-Assisted Infraclavicular Brachial Plexus Catheter Placement:

Implications of a New Technology. *Anesthesiology Research and Practice*. 2010;2010:1-4. doi:10.1155/2010/208025

4. Cool D, Sherebrin S, Izawa J, Chin J, Fenster A. In vitro validation of a 3-dimensional transrectal ultrasound system for prostate biopsiess. *CIM*. 2007;30(4):77. doi:10.25011/cim.v30i4.2846

5. Kishimoto J, Fenster A, Lee DSC, de Ribaupierre S. In Vivo Validation of a 3-D Ultrasound System for Imaging the Lateral Ventricles of Neonates. *Ultrasound in Medicine & Biology*. 2016;42(4):971-979. doi:10.1016/j.ultrasmedbio.2015.11.010

6. Zhang Y, Jordan JM. Epidemiology of Osteoarthritis. *Clinics in Geriatric Medicine*. 2010;26(3):355-369. doi:10.1016/j.cger.2010.03.001

7. Glyn-Jones S, Palmer AJR, Agricola R, et al. Osteoarthritis. *The Lancet*. 2015;386(9991):376-387. doi:10.1016/S0140-6736(14)60802-3

8. Swain S, Sarmanova A, Coupland C, Doherty M, Zhang W. Comorbidities in Osteoarthritis: A Systematic Review and Meta-Analysis of Observational Studies. *Arthritis Care Res*. 2020;72(7):991-1000. doi:10.1002/acr.24008

9. Louati K, Vidal C, Berenbaum F, Sellam J. Association between diabetes mellitus and osteoarthritis: systematic literature review and meta-analysis. *RMD Open*. 2015;1(1):e000077-e000077. doi:10.1136/rmdopen-2015-000077

10. Hall A, Stubbs B, Mamas M, Myint P, Smith T. Association between osteoarthritis and cardiovascular disease: Systematic review and meta-analysis. *European Journal of Preventive Cardiology*. 2016;23(9):938-946. doi:doi:10.117/2047487315610663

11. Haugen IK, Englund M, Aliabadi P, et al. Prevalence, incidence and progression of hand osteoarthritis in the general population: the Framingham Osteoarthritis Study. *Annals of the Rheumatic Diseases*. 2011;70(9):1581-1586. doi:10.1136/ard.2011.150078

12. Dahaghin S. Prevalence and pattern of radiographic hand osteoarthritis and association with pain and disability (the Rotterdam study). *Annals of the Rheumatic Diseases*. 2005;64(5):682-687. doi:10.1136/ard.2004.023564

13. Thompson JC, Netter FH (Frank H. *Netter's Concise Atlas of Orthopaedic Anatomy*. 1st ed. Icon Learning Systems; 2002.

14. Gillis J, Calder K, Williams J. Review of Thumb Carpometacarpal Arthritis Classification, Treatment and Outcomes. *Canadian Journal of Plastic Surgery*. 2011;19(4):134-138. doi:10.1177/229255031101900409

15. Smith MD, Wechalekar MD. The synovium. In: *Rheumatology*. Elsevier; 2015:27-32. doi:10.1016/B978-0-323-09138-1.00004-8

16. D. Smith M. The Normal Synovium. *TORJ*. 2011;5(1):100-106. doi:10.2174/1874312901105010100

17. Arden Nigel, Blanco Francisco, Cooper C, et al. *Atlas of Osteoarthritis [Electronic Resource]*. 1st ed. 2014. Springer Healthcare Ltd.; 2014. doi:10.1007/978-1-910315-16-3

18. Sonne-Holm S, Jacobsen S. Osteoarthritis of the first carpometacarpal joint: a study of radiology and clinical epidemiology. *Osteoarthritis and Cartilage*. 2006;14(5):496-500. doi:10.1016/j.joca.2005.12.001

19. Kessler S, St�ve J, Puhl W, St�rmer T. First carpometacarpal and interphalangeal osteoarthritis of the hand in patients with advanced hip or knee OA. Are there differences in the aetiology? *Clinical Rheumatology*. 2003;22(6):409-413. doi:10.1007/s10067-003-0783-5

20. Woolf A, Pfleger B. Burden of major musculoskeletal conditions. *Bull World Health Organ*. 2003;81:646-656.

21. Menon J. The problem of trapeziometacarpal degenerative arthritis. *Clin Orthop Relat Res*. 1983;(175):155-165.

22. Van Heest AE, Kallemeier P. Thumb Carpal Metacarpal Arthritis: *Journal of the American Academy of Orthopaedic Surgeons*. 2008;16(3):140-151. doi:10.5435/00124635-200803000-00005

23. Barron OA, Eaton RG. Save the trapezium: Double interposition arthroplasty for the treatment of stage IV disease of the basal joint. *The Journal of Hand Surgery*. 1998;23(2):196-204. doi:10.1016/S0363-5023(98)80114-7

24. Wolf JM, Oren TW, Ferguson B, Williams A, Petersen B. The Carpometacarpal Stress View Radiograph in the Evaluation of Trapeziometacarpal Joint Laxity. *The Journal of Hand Surgery*. 2009;34(8):1402-1406. doi:10.1016/j.jhsa.2009.06.030

25. Clancey GJ. Radiograph Assessment of the Basal Thumb Joint: *Orthopaedic Nursing*. 1989;8(4):58-59. doi:10.1097/00006416-198907000-00021

26. Bijlsma JW, Berenbaum F, Lafeber FP. Osteoarthritis: an update with relevance for clinical practice. *The Lancet*. 2011;377(9783):2115-2126. doi:10.1016/S0140-6736(11)60243-2

27. Kennedy CD, Manske MC, Huang JI. Classifications in Brief: The Eaton-Littler Classification of Thumb Carpometacarpal Joint Arthrosis. *Clinical Orthopaedics & Related Research*. 2016;474(12):2729-2733. doi:10.1007/s11999-016-4864-6

28. Pelletier JP, Martel-Pelletier J, Abramson SB. Osteoarthritis, an inflammatory disease: Potential implication for the selection of new therapeutic targets. *Arthritis & Rheumatism*. 2001;44(6):1237-1247. doi:10.1002/1529-0131(200106)44:6<1237::AID-ART214>3.0.CO;2-F

29. Loeuille D, Chary-Valckenaere I, Champigneulle J, et al. Macroscopic and microscopic features of synovial membrane inflammation in the osteoarthritic knee: Correlating magnetic resonance imaging findings with disease severity. *Arthritis Rheum*. 2005;52(11):3492-3501. doi:10.1002/art.21373

30. Myers SL, Brandt KD, Ehlich JW, et al. Synovial inflammation in patients with early osteoarthritis of the knee. *J Rheumatol*. 1990;17(12):1662-1669.

31. Benito MJ. Synovial tissue inflammation in early and late osteoarthritis. *Annals of the Rheumatic Diseases*. 2005;64(9):1263-1267. doi:10.1136/ard.2004.025270

32. Haraoui B, Pelletier JP, Cloutier JM, Faure MP, Martel-Pelletier J. Synovial membrane histology and immunopathology in rheumatoid arthritis and osteoarthritis. In vivo effects of antirheumatic drugs. *Arthritis & Rheumatism*. 1991;34(2):153-163. doi:10.1002/art.1780340205

33. Wenham CYJ, Conaghan PG. The role of synovitis in osteoarthritis. *Therapeutic Advances in Musculoskeletal*. 2010;2(6):349-359. doi:10.1177/1759720X10378373

34. Zhang W, Moskowitz RW, Nuki G, et al. OARSI recommendations for the management of hip and knee osteoarthritis, Part I: Critical appraisal of existing treatment guidelines and systematic review of current research evidence. *Osteoarthritis and Cartilage*. 2007;15(9):981-1000. doi:10.1016/j.joca.2007.06.014

35. Zhang W, Moskowitz RW, Nuki G, et al. OARSI recommendations for the management of hip and knee osteoarthritis, Part II: OARSI evidence-based, expert consensus guidelines. *Osteoarthritis and Cartilage*. 2008;16(2):137-162. doi:10.1016/j.joca.2007.12.013

36. Zhang W, Nuki G, Moskowitz RW, et al. OARSI recommendations for the management of hip and knee osteoarthritis. *Osteoarthritis and Cartilage*. 2010;18(4):476-499. doi:10.1016/j.joca.2010.01.013

37. Jordan KM. EULAR Recommendations 2003: an evidence based approach to the management of knee osteoarthritis: Report of a Task Force of the Standing Committee for International Clinical Studies Including Therapeutic Trials (ESCISIT). *Annals of the Rheumatic Diseases*. 2003;62(12):1145-1155. doi:10.1136/ard.2003.011742

38. Zhang W. EULAR evidence based recommendations for the management of hip osteoarthritis: report of a task force of the EULAR Standing Committee for International Clinical Studies Including Therapeutics (ESCISIT). *Annals of the Rheumatic Diseases*. 2005;64(5):669-681. doi:10.1136/ard.2004.028886

39. Kolasinski SL, Neogi T, Hochberg MC, et al. 2019 American College of Rheumatology/Arthritis Foundation Guideline for the Management of Osteoarthritis of the Hand, Hip, and Knee. *Arthritis Rheumatol*. 2020;72(2):220-233. doi:10.1002/art.41142

40. Tsehaie J, Porsius JT, Rizopoulos D, et al. Response to Conservative Treatment for Thumb Carpometacarpal Osteoarthritis Is Associated With Conversion to Surgery: A Prospective Cohort Study. *Physical Therapy*. Published online January 30, 2019. doi:10.1093/ptj/pzz009

41. Bannwarth B. Acetaminophen or NSAIDs for the treatment of osteoarthritis. *Best Practice & Research Clinical Rheumatology*. 2006;20(1):117-129. doi:10.1016/j.berh.2005.09.004

42. Zhang W, Jones A, Doherty M. Does paracetamol (acetaminophen) reduce the pain of osteoarthritis?: a meta-analysis of randomised controlled trials. *Ann Rheum Dis*. 2004;63(8):901. doi:10.1136/ard.2003.018531

43. Caldwell JR. Intra-Articular Corticosteroids: Guide to Selection and Indications for Use. *Drugs*. 1996;52(4):507-514. doi:10.2165/00003495-199652040-00004

44. Mayer JH. CARPOMETACARPAL OSTEOARTHRITIS OF THE THUMB. *The Lancet*. 1970;296(7666):270. doi:10.1016/S0140-6736(70)92628-0

45. Bahadır C, Onal B, Dayan VY, Gürer N. Comparison of therapeutic effects of sodium hyaluronate and corticosteroid injections on trapeziometacarpal joint osteoarthritis. *Clin Rheumatol*. 2009;28(5):529-533. doi:10.1007/s10067-008-1079-6

46. Day CS, Gelberman R, Patel AA, Vogt MT, Ditsios K, Boyer MI. Basal joint osteoarthritis of the thumb: a prospective trial of steroid injection and splinting. *The Journal of Hand Surgery*. 2004;29(2):247-251. doi:10.1016/j.jhsa.2003.12.002

47. Eaton RG, Glickel SZ. Trapeziometacarpal osteoarthritis. Staging as a rationale for treatment. *Hand Clin*. 1987;3(4):455-471.

48. Angwin J, Heald G, Lloyd A, Howland K, Davy M, James MF. Reliability and sensitivity of joint space measurements in hand radiographs using computerized image analysis. *J Rheumatol*. 2001;28(8):1825-1836.

49. Huétink K, van 't Klooster R, Kaptein BL, et al. Automatic radiographic quantification of hand osteoarthritis; accuracy and sensitivity to change in joint space width in a phantom and cadaver study. *Skeletal Radiol*. 2012;41(1):41-49. doi:10.1007/s00256-011-1110-x

50. Thoenen J, MacKay JW, Sandford HJC, Gold GE, Kogan F. Imaging of Synovial Inflammation in Osteoarthritis, From the *AJR* Special Series on Inflammation. *American Journal of Roentgenology*. 2022;218(3):405-417. doi:10.2214/AJR.21.26170

51. Haugen IK, Østergaard M, Eshed I, et al. Iterative Development and Reliability of the OMERACT Hand Osteoarthritis MRI Scoring System. *J Rheumatol*. 2014;41(2):386-391. doi:10.3899/jrheum.131086

52. Ogbole GI, Adeyomoye AO, Badu-Peprah A, Mensah Y, Nzeh DA. Survey of magnetic resonance imaging availability in West Africa. *Pan Afr Med J*. 2018;30:240. doi:10.11604/pamj.2018.30.240.14000

53. Kaeley GS, Bakewell C, Deodhar A. The importance of ultrasound in identifying and differentiating patients with early inflammatory arthritis: a narrative review. *Arthritis Res Ther*. 2020;22(1):1. doi:10.1186/s13075-019-2050-4

54. Epis O, Paoletti F, d'Errico T, et al. Ultrasonography in the diagnosis and management of patients with inflammatory arthritides. *European Journal of Internal Medicine*. 2014;25(2):103-111. doi:10.1016/j.ejim.2013.08.700

55. Wakefield RJ, Balint PV, Szkudlarek M, et al. Musculoskeletal ultrasound including definitions for ultrasonographic pathology. *J Rheumatol*. 2005;32(12):2485-2487.

56. McNally EG. Ultrasound of the small joints of the hands and feet: current status. *Skeletal Radiol*. 2008;37(2):99-113. doi:10.1007/s00256-007-0356-9

57. D'Agostino MA, Terslev L, Aegerter P, et al. Scoring ultrasound synovitis in rheumatoid arthritis: a EULAR-OMERACT ultrasound taskforce — Part 1: definition and development of a standardised, consensus-based scoring system. *RMD Open*. 2017;3(1):e000428. doi:10.1136/rmdopen-2016-000428

58. Fenster A, Downey DB, Cardinal HN. Three-dimensional ultrasound imaging. *Phys Med Biol*. 2001;46(5):R67-R99. doi:https://doi.org/10.1088/0031-9155/46/ 5/201.

59. Prager RW, Ijaz UZ, Gee AH, Treece GM. Three-dimensional ultrasound imaging. *Proc Inst Mech Eng H*. 2010;224(2):193-223. doi:10.1243/09544119JEIM586

60. Kim YJ, Wolf PD. 3-D Ultrasound Imaging Using Helicoid Array Transducers. *IEEE Trans Ultrason, Ferroelect, Freq Contr*. 2021;68(3):697-706. doi:10.1109/TUFFC.2020.3022616

61. Smith WL, Fenster A. Optimum scan spacing for three-dimensional ultrasound by speckle statistics. *Ultrasound in Medicine & Biology*. 2000;26(4):551-562. doi:10.1016/S0301-5629(99)00162-3

62. Sam Papernick, Derek J. Gillies, Tom Appleton, Aaron Fenster. Three-dimensional ultrasound for monitoring knee inflammation and cartilage damage in osteoarthritis and rheumatoid arthritis. In: Vol 11315. ; 2020. https://doi.org/10.1117/12.2549624

63. Papernick S, Dima R, Gillies DJ, Appleton CT, Fenster A. Reliability and concurrent validity of three-dimensional ultrasound for quantifying knee cartilage volume. *Osteoarthritis and Cartilage Open*. 2020;2(4):100127. doi:https://doi.org/10.1016/j.ocarto.2020.

Chapter 2

2 Three-Dimensional Ultrasound to Investigate Synovitis in the Hand and Wrist

The purpose of Chapter 2 is to present the validation and rater reliability of a semi-submerged mechanical 3D US scanning device for measuring CMC1 synovial tissue volume compared to the gold standard of MRI. In this chapter, we discuss the linear and volumetric validation of the device and examine its validity and reliability compared to the clinical gold standard of MRI using 10 CMC1 OA patients.

The contents of this chapter have been submitted to the journal of Medical Physics and is currently under review for publication.

2.1 Introduction

As stated in Chapter 1, Osteoarthritis (OA) is now considered a progressive joint disease characterized by inflammation of the synovium, degradation of the articular cartilage, and abnormal changes to the subchondral bone[1]. OA is considered the most common form of arthritis, affecting 1 in 7 North American adults, and its prevalence is projected to continue to rise with the increasing trend in population age and body mass index (BMI).[2,3] Hand osteoarthritis (HOA) is the cause of considerable pain and disability, leading to the inability to perform activities of daily living and ultimately decreasing the quality of life for many individuals.[4,5] Epidemiological studies of elderly populations have estimated that the prevalence of HOA ranges from 44% to as high as 92% and is more commonly seen in women than men[6,7,8].

One of the most common sites for HOA is the carpometacarpal joint of the thumb, causing considerable disability as proper thumb motion is required for almost all activities of daily living. Despite the considerable impact of HOA on patients' lives, there are fewer studies conducted on

the hands compared to larger joints such as the knee, and most of these studies focused on radiographic OA instead of symptomatic OA.[9] Although radiographs are the most common imaging modality used to diagnose and monitor OA, multiple studies have reported discrepancies between radiographic severity and patient symptoms, as some patients display no radiographic damage but still present with symptoms such as pain.[10,11] This is due to radiographs inability to capture subtle changes in early-stage OA due to the lack of soft-tissue contrast.[12]

Over the last two decades, interest has increased in understanding the role of soft tissue structures in symptomatic OA. Studies have demonstrated that chronically elevated levels of the inflammatory mediators associated with synovitis can lead to cartilage degradation and breakdown of underlying subchondral bone.[14] Although the degree of inflammation observed in OA is not as extensive as rheumatoid arthritis (RA), synovial effusions and membrane hypertrophy are now more frequently associated with OA due to the use of more sensitive imaging modalities such as magnetic resonance imaging (MRI) and two-dimensional ultrasound imaging (2-D US).[14] As mentioned in Chapter 1, MRI has been shown to have adequate sensitivity for characterizing tissue damage and degeneration but is associated with many significant limitations including cost, time efficiency, and accessibility. Additionally, to provide a comprehensive assessment of inflammatory activity, contrast-enhanced MRI is recommended, which carries the additional risk of gadolinium toxicity and nephrogenic systemic fibrosis.[13]

Two-dimensional musculoskeletal ultrasound (2-D US) has been reported as a reliable method of imaging synovial tissue changes in patients with OA and RA.[16] Additionally, US imaging systems are inexpensive, readily available, and exams can be conducted at the patient's bedside. Studies have examined the relationship of US findings with symptoms and functions in hand OA and other joints such as the hip and knee.[17,18,19] However, 2-D US presents significant

limitations, as discussed in detail in Chapter 1 of this thesis. The need for operators to mentally transform 2-D images to 3-D impressions of the anatomy and the dependency on transducer position and location are two limitations that make musculoskeletal US imaging challenging.

Three-dimensional US (3-D US) technology is an attractive alternative to 2-D US for quantifying and monitoring changes in OA as it can overcome many of the limitations associated with 2-D US imaging.[20] Currently, there are three main methods for 3D US image acquisition, each of which has its own advantages and limitations for use in imaging of HOA. The first approach uses 2-D array transducers, which generate an acoustic beam in both the elevational and azimuth dimensions, allowing it to obtain a three-dimensional image. 2-D array transducers have been used extensively in abdominal and obstetrical imaging, but musculoskeletal purposes such as soft-tissue and nerve functioning have been few.[21,22,23] However, the frequency of standard commercial 2-D array transducers is 8.5MHz, which is much lower than transducers commonly used for musculoskeletal imaging (8-18 MHz). Additionally, commercial systems with 2-D arrays generally do not provide an easy method to export the 3D US image to be used for further analysis. An alternative 3D US imaging method uses freehand scanning, in which the conventional transducer's position and orientation are tracked using an optical or electromagnetic sensor as it is moved over the anatomy.[20] The advantage of this method is that it allows clinicians to manipulate the transducer in the normal manner. However, it relies on the operator's skill, and the approach requires somewhat costly tracking hardware that may be limited due to environmental factors (ferromagnetic materials and optical line of sight). Most importantly, it does not guarantee that the region of the anatomy is in the same position at a later session if the region is mobile (e.g., hand and thumb). The third method consists of translating a conventional 2-D US transducer using a motorized drive mechanism, allowing integration of any

manufacturer's transducer into a drive mechanism that is simple and inexpensive. This method has been used in various studies examining the feasibility of using 3D US to investigate cardiac, oncological, and pediatric pathologies,[25,26,27] There have only been a few studies that reported the use of 3D US for musculoskeletal imaging, and even fewer that focus on HOA and characterization of synovial volume.[28,29,30,32,33] Chauvin and Doria suggested the use of a mechanically translated 3D US device to examine synovial inflammation in juvenile idiopathic arthritis; however, no results of this proposed study have been published to date.[29] Papernick et al., used a similar mechanically translated scanning approach to acquire images of healthy knee cartilage. This handheld device with a 10 MHz linear transducer worked well for large and flat regions of the anatomy, such as the knee.[28] However, this approach suffers from signal loss due to inadequate coupling of the US transducer to the anatomy in complex surfaces such as the hand and thumb. Therefore, the development and validation of a 3D US device for smaller joints and with complex surfaces such as those found in the hand and wrist is needed to provide an inexpensive and rapid method to solve this unmet clinical need.

In this chapter, we describe a new system for generating 3D US images of the hand and wrist. This system includes a custom motorized US transducer mover, 3D US reconstruction software, and a positioning device designed specifically to standardize the hand position between subsequent scanning sessions and modalities. The objectives of this chapter are to (1) assess the linear and volumetric measurements capabilities of the proposed 3D US machine using imaging phantoms, (2) validate and measure the precision of 3D US-based measures of synovial tissue volume using gold standard MRI-based measurements in CM1 OA, and (3) to evaluate the intra- and inter-rater reliability of our manual synovial tissue volume measurements.

2.2 Methods

2.2.1 3-Dimensional Ultrasound System

The mechanical 3D US acquisition device was developed to allow imaging of the hands and wrists, which have complex surfaces, and to provide a method to position the hand and wrists in the same position and orientation in subsequent imaging sessions. Our device makes use of a motorized submerged transducer moving assembly (mover) designed specifically for use inside a wrist positioning container, which consists of an 11-liter tank filled with a 7.25% isopropyl alcohol solution to match the speed of sound of tissue (1540 m/s)[34] (Fig. 2.2.1.1). This mover is compatible with any commercially available 2-D US machine and linear US transducer and housed in a custom 3-D printed attachment, but for this study, a Canon Aplio i700 US machine (Canon Medical Systems, Tustin, California, US) and a 14L-5 linear transducer with a 10 MHz operating frequency (3.8MHz – 10.0MHz) and 58 mm footprint. To obtain a 3D US image, the transducer can be translated up to 30 cm linearly within the submersion tank by a Micromo Rotary Coreless DC 1331T 006 SR motor (MicroMo Electronics, Clearwater, FL, USA) with an integrated electromagnetic encoder, which records the rotational position of the motor. This motor is powered by a 12V DC power supply, which is controlled by a Micromo MCDC 3006S motor controller linked to a desktop workstation through a USB connection. An Epiphan DVI2USB3.0 video frame grabber (Epiphan Systems Inc., Ottawa, ON, Canada) connected to the digital visual interface port of the 2-D US machine transmits the images to a computer workstation. The system acquires a series of 2-D images at 0.166 mm spatial intervals at a 20.3 Hz rate, and the acquired 2D US images are reconstructed into a 3D US image (0.114 x 0.114 x 0.333 mm^3 voxel size) as 324 2D US images are acquired. Typically, the scan length and time were 8.12 cm and 16 sec for imaging the thumb.

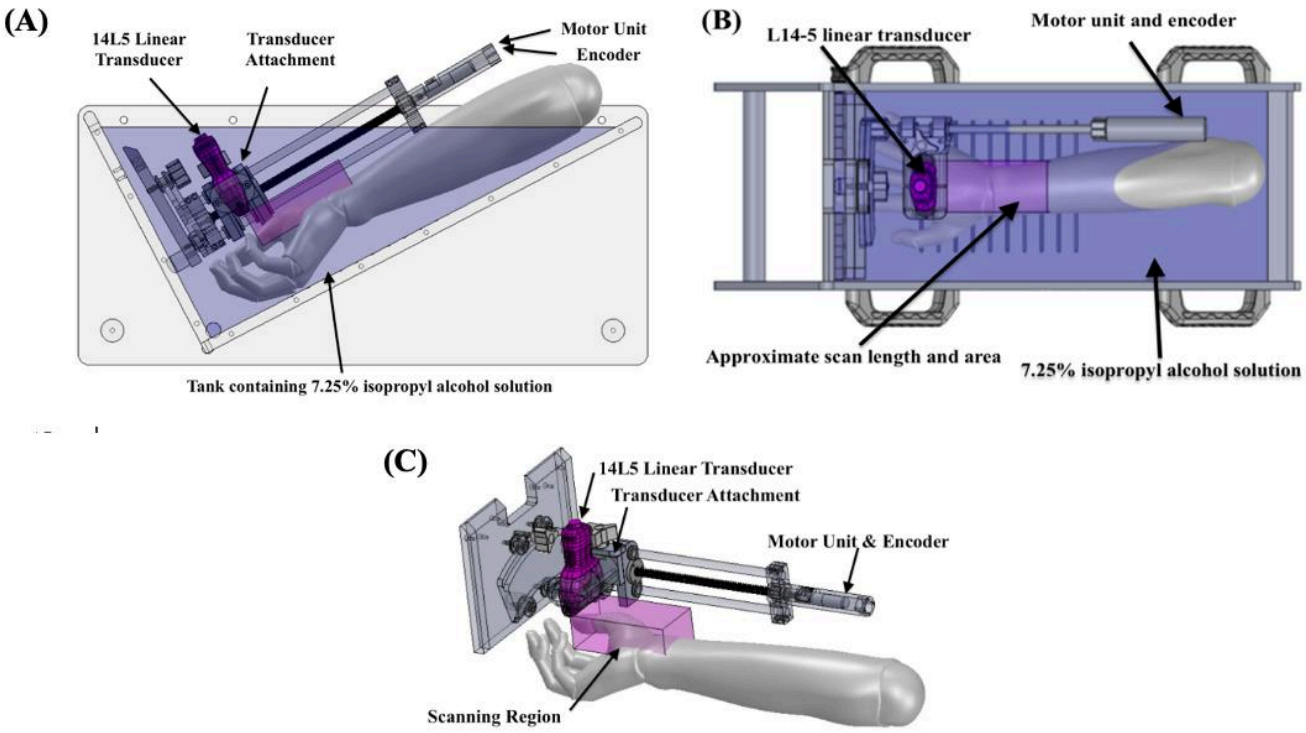

Figure 2.2.1.1: Schematics of the 3D US hand imaging device. This figure shows **(**A) side view of the 3D US scanning device showing hand placement, 14L-5 linear US probe, motor unit, and 7.25% isopropyl alcohol solution. (B) Top view of the submerged mechanical 3D US scanning device. (C) Side view of the mechanical components of the 3D US device.

2.2.2 Wrist Positioning Device:

A wrist positioning device was fabricated to allow standardizing of the hand position between imaging modalities (i.e., 3D US and MRI) and subsequent scanning sessions. The positioning device is composed of polycarbonate two plates, attached at a 120° angle as seen in Fig. 2.2.2.2. Each patient's hand was locked in place by a series of Delrin pegs that allowed for consistent hand positioning between the MR and 3D US imaging sessions. The configuration of the pegs was recorded and was specific to the patient's hand size.

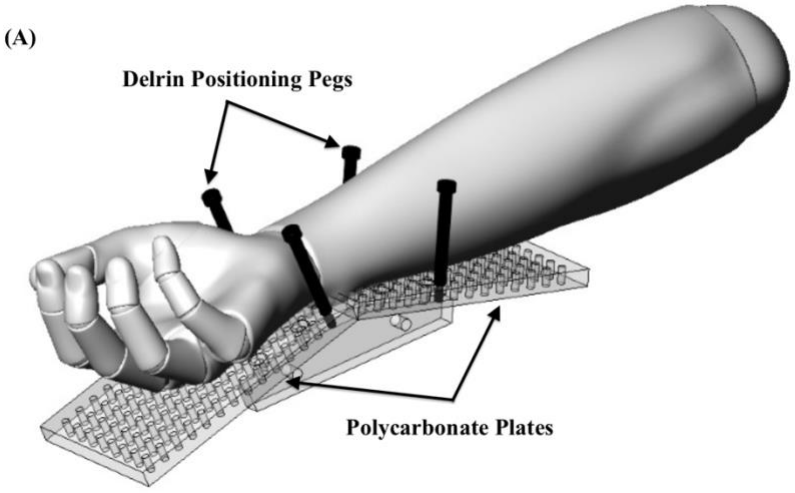

Figure 2.2.1.2: Wrist positioning device. This device was used for standardizing patient position in 3D US and MRI. The image includes two polycarbonate plates, Delrin positioning pegs, and the scanning position for the CMC1 patients. A grid of small holes in the polycarbonate plates was used to assist in stabilizing the hand position.

2.2.3 Linear Validation of Image Reconstruction

To evaluate the accuracy of the reconstructed 3D US geometry, a multilayer monofilament string-grid phantom (Fig. 2.3.1.1) (10 mm square grid) was scanned in a 7.25% isopropyl alcohol (Sigma Aldrich, Co., St. Louis, MO, USA) solution to provide the correct speed-of-sound of soft tissues (1540 m/s). The string layers of this phantom were offset to prevent shadowing, which resulted in diagonal distances between strings of 10.3 mm and 12.5 mm. The distances between the intersections of the strings in each coordinate plane of the reconstructed images were then measured manually using image visualization and processing software (3D Slicer 4.11.0 Preview Release). The mean measurement [N= 36, 36, 32 for the x-direction, y-direction, z-direction] for each coordinate plane was then compared to the physical known distances (i.e., 10.0 mm, 10.3 mm, and 12.5 mm).

2.2.4 Volume Validation:

To validate the volumetric measurement capabilities of the system, a simulated synovial tissue phantom with an embedded synovial effusion was fabricated and imaged using the 3D US device. The phantom was developed to represent an anatomically correct CMC1 joint. The simulated synovium phantom was comprised of agar and 3-D printed nylon bones. The simulated synovial membrane and effusion were constructed using the tip of a surgical glove, filled with 1300 mm^3 of tissue-mimicking agar (200 mL water, 16 mL glycerol, 7 g agar powder, 3g sigmacell cellulose) (Sigma Aldrich, Co., St. Louis, MO, USA). The tips of the glove were sealed with hot melting adhesive. Previously acquired CT images of a first metacarpal and trapezium were used as the models to 3-D print the bone components. The simulated effusion and the 3-D printed bones were placed in the anatomically correct positions and then covered in background tissue-simulating agar containing sigmacell cellulose scattering agent (35 g agar

powder, 1000 ml distilled water, 80 ml glycerol, 15 g sigmacell cellulose). This was done to mimic soft-tissue scatter in the US images and provide contrast between the background and synovial effusions mimics.

To test the inter- and intra-rater variability of the segmented volumes, the phantom was scanned, and then the 3-D images were repeatedly segmented by two raters ten times with a 24-hour washout period. The 3D US images were analyzed using 3-D Slicer (3D Slicer 4.11.0 Preview Release) by manually segmenting the simulated effusion observed in individual 3-D image slices. To establish segmentation boundaries, the two raters identified the most medial and lateral edges of the embedded object and segmented all visible areas of the simulated effusion using every second slice. These slices were spaced 0.33 mm apart in the in-plane (transverse) image. These individual slices were then interpolated using 3D Slicer software to form a 3-D model of the embedded simulated effusion. The known physical volume of the simulated effusion (1300 mm^3) was obtained using the water displacement method. Measurements were repeated three times, and the mean volume was used in our comparisons to the image-based volume measurements.

2.2.5 Clinical Validation

The imaging protocol for this study was approved by the Research Ethics Board at Western University (Ontario, Canada) and all patients provided written informed consent prior to taking part in this study. We imaged ten CMC1 OA patients to determine the utility of our 3D US system for measuring joint synovium volumes. Patients were diagnosed as having CMC1 OA by a hand surgeon at the Roth | McFarlane Hand and Upper Limb Center (London, Canada). 3D US images were acquired of the CMC1 OA patients on the ventral side of the hand, with the thenar eminence facing the transducer. Since MRI is the current clinical gold standard,

complimentary MR images were acquired with a GE Discovery MR750 3.0T whole-body system (General Electric Healthcare, Milwaukee, WI, USA) using Photon Density Fast-Spin Echo with Fat Saturation sequence for comparison. A 32-channel carotid coil (NeoCoil, Pewaukee, WI, USA) was used while patients were positioned on the MRI bed in the full-body prone and full shoulder flexion position with their affected hand placed in the bore of the MRI machine. The hand was fixed in the previously described hand positioning device (Fig. 2.2.1.2) to standardize hand positioning between the 3D US device and MRI.

The two raters involved in this study had extensive backgrounds in anatomy and physiology and had received specialized training in MSK US. Additionally, rater 2 was a sonographer certified by Sonography Canada. The synovium was identified in each set of images, and the raters established segmentation boundaries as the most lateral and medial edges of the first metacarpal and trapezium bones. The volumes of the synovium observed in these regions were manually segmented using 0.33 mm distances between 3D image slices and all areas that exhibit hypoechoic character or hyperplasia of the membrane. To assess 3-D US- and MRI-based volume measurement reliability and accuracy, the images were segmented by two different trained raters using the methods previously described, and the measured volumes were compared. The average segmentation time was approximately 10 min once boundaries were established.

2.2.6 Statistical Analysis

Statistical analyses for all data were performed using SPSS (SPSS Statistics v26; IBM, Armonk, NJ). Distribution normality was assessed using the Shapiro-Wilk test. The significance level was chosen such that the probability of making a type I error was less than 5% ($p < 0.05$). The metrics used to assess the linear measurement capabilities of the system were the mean,

standard deviation, coefficient of variation, and percent error. These metrics were also used to compare the volumetric phantom measurements found using 3D US and MRI.

The accuracy and precision of the patient synovial volume measurements were assessed using the mean difference between MRI and 3-D US. In addition, SEM and Minimal Detectible Change (MDC at 95% confidence interval) were calculated from the repeated 3D US and MRI segmentation values to estimate measurement error and the threshold for true, statistically detectable change, respectively.[34] SEM and MDC are calculated using Eqs. 1 and 2, respectively.

$$SEM = SD_{pooled} \times \sqrt{(1 - ICC)} \quad (1)$$

$$MDC = 1.96 \times SEM \times (\sqrt{2}) \quad (2)$$

Intra- and inter- rater segmentation reliabilities from 3D US and MRI images of the CMC1 patients were assessed for both raters using intraclass correlation coefficients (ICCs Inter-rater ICCs were based on a single-rating, absolute-agreement, 2-way random-effects model, while intra-rater ICCs were based on single-rating, absolute-agreement, 2-way mixed-effects model). ICCs were interpreted as poor reliability for less than 0.50, moderate reliability for between 0.50 and 0.75, good reliability between 0.75 and 0.90, and excellent reliability for over 0.90[35]. Individual two-sample t-tests were used to determine if there were any statistically significant differences between the volumetric measurements observed by the two raters as well as between the measurements obtained with MRI and 3-D US.

We also examined the impact of synovial volume on segmentation variability by plotting the difference in repeated segmentation V_1 and V_2 normalized by the mean of the two volume measurements (i.e., relative delta Eq.3) as a function of the mean volume, thus:

$$\textit{Relative Delta} = \left|\frac{V_1 - V_2}{(V_1 + V_2)/2}\right| \quad (3)$$

2.3 Results

2.3.1 Linear Phantom Validation

Figure 2.3.1.1 shows a photograph of the string phantom and the corresponding 3D US image sliced to reveal the intersections of the strings. As shown in Table 1, the mean percent error for all measurements in all directions and planes ranged from 0.13% to 1.06% of the expected values. The largest percent error was observed in the Z direction of the (X, Z) plane, which is the reconstructed plane of the 3D US image.

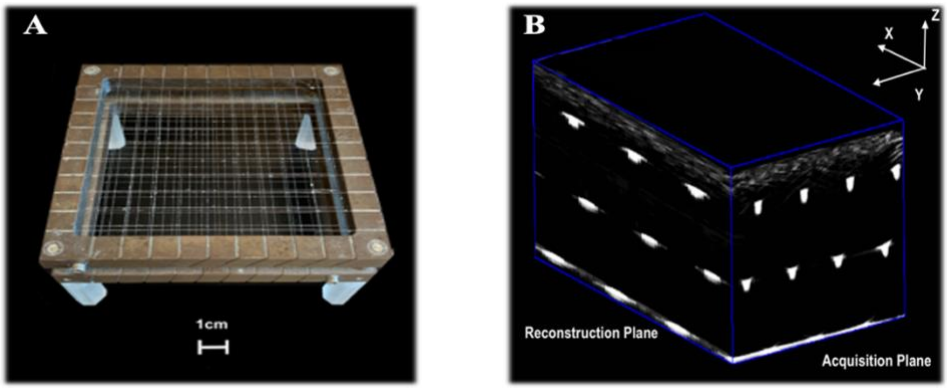

Figure 2.3.1.1: Linear Imaging Phantom. A multilayer grid phantom comprised of microfilament strings spaced 10.0 mm, 10.3 mm, and 12.5 mm apart and offset diagonally to prevent US shadowing (A). 3D US reconstruction, including labeled reconstruction and acquisition plane(B).

Table 2.3.1.1: Summary of distance measurements made in each coordinate plane of the 3D US image of the string phantom.

	(X, *Y*) Plane		(*X*, *Z*) Plane			(*Y*, *Z*) Plane		
	X	***Y***	***X***	***Z*₁**	***Z*₂**	***Y***	***Z*₁**	***Z*₂**
Expected Distance (mm)	10.0	10.0	10.0	12.5	10.3	10.0	12.5	10.3
Mean Distance (mm)	10.06	10.06	10.05	12.57	10.41	10.06	12.48	10.37
Standard Deviation (mm)	0.08	0.08	0.10	0.12	0.12	0.09	0.12	0.05
Error (%)	0.60%	0.60%	0.50%	0.56%	1.06%	0.60%	0.13%	0.63%
N	20	20	16	8	8	16	8	8

2.3.2 Volumetric Phantom Validations

Figure 2.3.2.1 shows the synovial tissue-mimicking phantom and a 3D US image. The mean 3D US-based volumetric measurement observed for all the CMC1 phantom segmentations was 1323.37 ± 25.13 mm^3, which was 1.8% larger than the known physical volume of 1300 mm^3. A two-sided t-test comparing the two raters and the image-based volume to the known volume showed no statistically significant difference between the mean volumes. The coefficient of variation for raters 1 and 2 were 0.8% and 2.6%, respectively. The mean Dice similarity coefficient (DSC) between the two raters was 88.0% with a mean Hausdorff distance (HD) of 0.34 ± 0.17 mm.

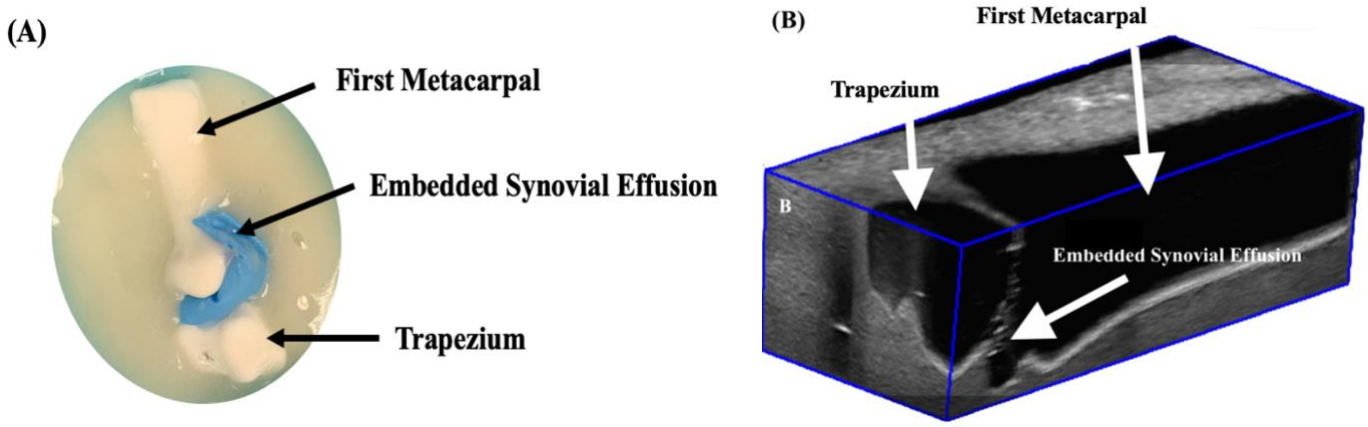

Figure 2.3.2.1: Anatomical Volumetric Imaging Phantom. (A) The tissue simulating volumetric phantom for the CMC1 joint and (B) its reconstructed 3D US image, showing the first metacarpal, trapezium, and the embedded synovial effusion.

2.3.3 Clinical Validation

Table 2.3.3.2 summarizes the patient demographic information and Eaton-Littler Grade for the classification of radiographic CMC1 OA of the patients we imaged. Eaton-Littler grades were assigned by an experienced orthopedic surgeon at the Roth|McFarlane Hand and Upper Limb Centre (London, Ontario). Figure 2.3.3.1 shows 3D US and MRI images of the CMC1 joint of three patients with mild, medium, and severe synovitis. The mean differences for the CMC1 patient volume measurements observed between the two raters were 2.61± 24.71 mm^3 (3D US) and 13.85 ± 9.04 mm^3 (MRI). The difference between 3D US and the gold standard MRI was 1.78%. A two-sided t-test showed no statistically significant difference in the volume measurements found using 3D US and MRI in the CMC1. The correspondence between the 3D US and MRI volume measurements can be seen in the linear regression and Bland-Alman plots in Fig. 7A and 7B. These plots indicate a high correspondence and a small bias of -5.89 mm^3. The difference between the two repeated 3D US synovial tissue volume measurements showed

an SEM of 11.21 mm^3 and an MDC of 31.06 mm^3, while the difference between MRI synovial tissue volume measurements demonstrated an SEM of 16.82 mm^3 and an MDC of 46.63 mm^3**.**

The relationship between CMC1 patient synovial tissue volume and segmentation variation (i.e., relative delta, Eq. 3) for 3D US and MRI are shown Fig. 8A and 8B. These plots indicate an increase in segmentation variation when segmenting smaller and larger synovial tissue volumes for both 3D US and MRI.

Table 2.3.3.1: Summary of patient demographics and Eaton- Littler Grade

Age (mean ± SD)	66.25 ± 7.08
Female/male	4/6
Eaton-Littler Grade	
Grade 0	0
Grade 1	0
Grade 2	3
Grade 3	4
Grade 4	1

As previously discussed in the section 2.2.6, the ICC values are to be interpreted as <0.5 equals poor reliability, between 0.5 and 0.75 as moderate reliability, and between 0.75 and 0.9 as good reliability. ICC values greater than 0.9 indicate excellent reliability based on guidelines provided by Koo and Li[35].The inter-rater ICC for the 3D US and MRI CMC1 synovial volumes was 0.94 and 0.99, and the intra-rater values were 0.99 and 0.99, respectively. Determining the DSC between MRI and 3D US patient segmentations was not feasible as slight differences in

patient's hand movement during the patient moving from the 3D US imaging suite to the MRI scanner and compression in the MRI coil led to variation in the structure of the synovial membrane and the fluid effusion within, but the volumes were not affected.

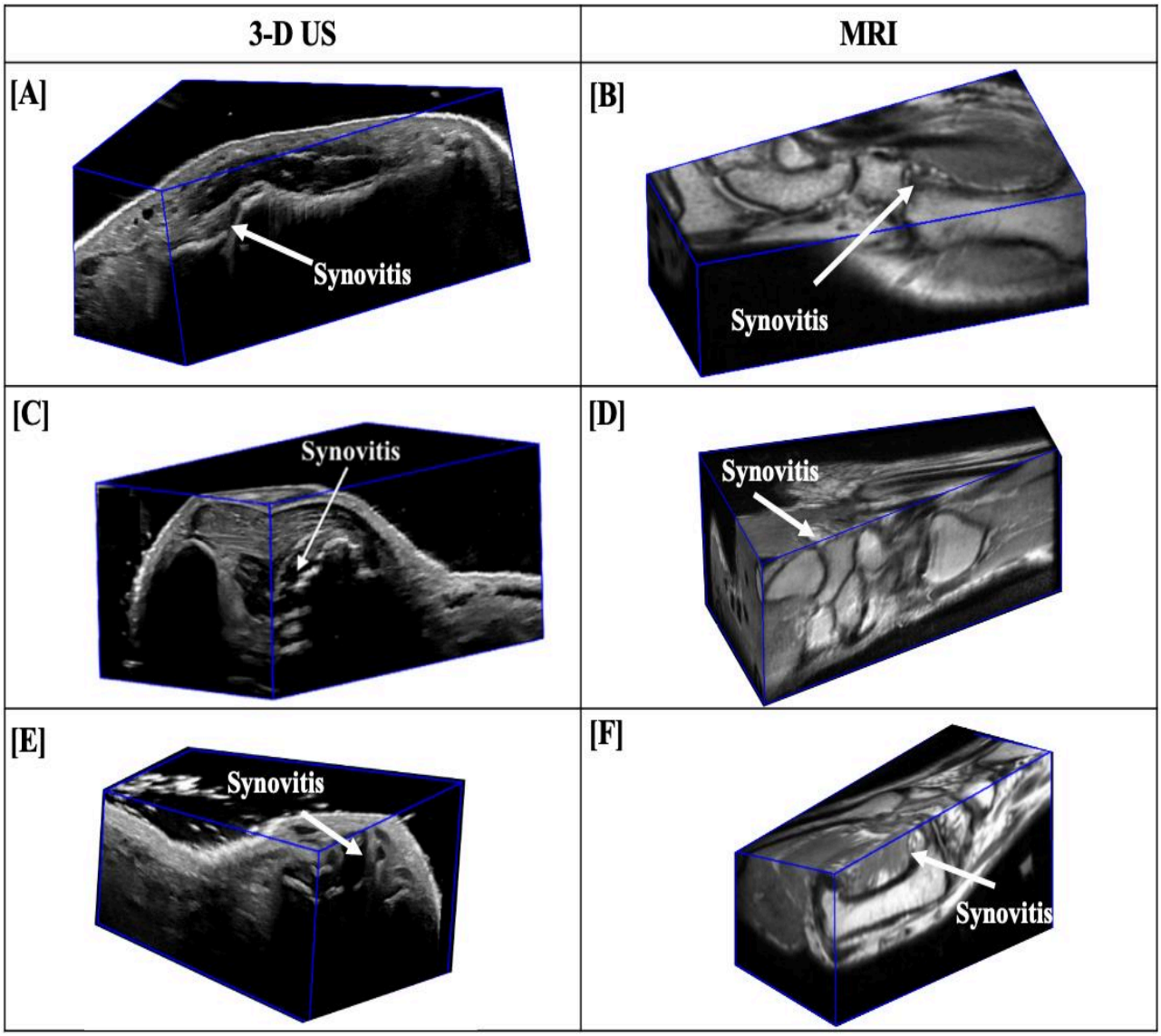

Figure 2.3.3.1: MRI and 3D US images of the CMC1 joint of patients with synovitis. 3D US (A) and MRI (B) of a patient with mild synovitis (114.10 mm^2). 3D US (C) and MRI (D) of a patient with medium synovitis (372.57 mm^2). 3D US (E) and MRI (F) of a patient with severe synovitis (605.99 mm^2). In MRI, synovial tissue appears as bright structures extending from the joint. In comparison, in US we see synovitis represented in anechoic sections (black) due to the way the acoustic waves are bounced back to the transducer. Segmenting MRI is challenging due to the increased field of view but decreased spatial resolution.

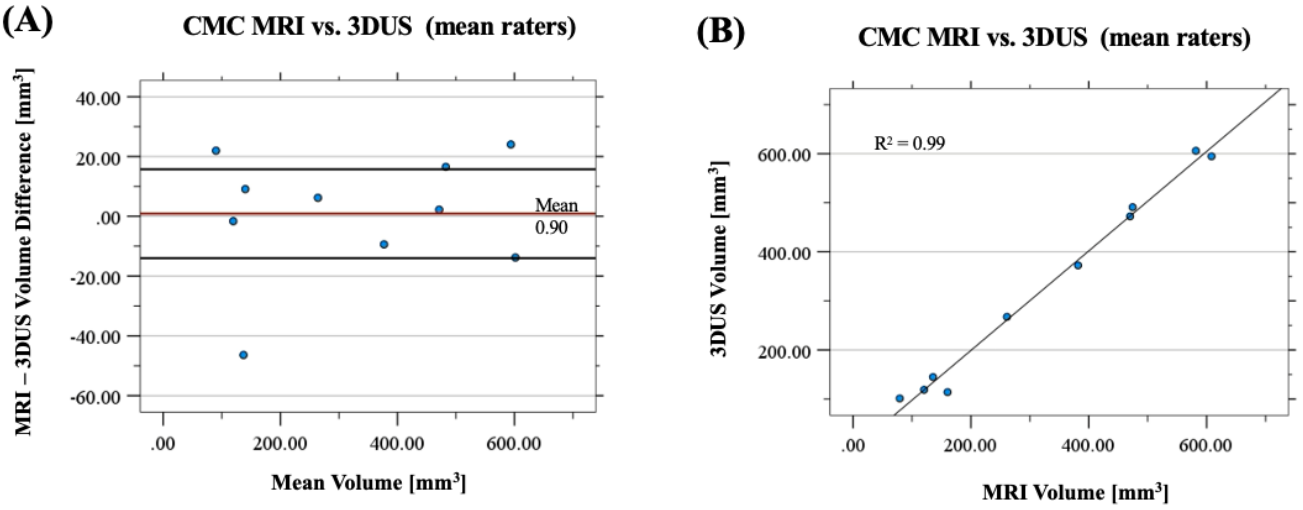

Figure 2.3.3.2: Bland-Altman and Linear Regression plots. Bland-Altman plot assessing the relationship between CMC 3DUS and MRI (A). Linear regression plots of MRI segmentation volumes used as predictors for 3DUS (B).

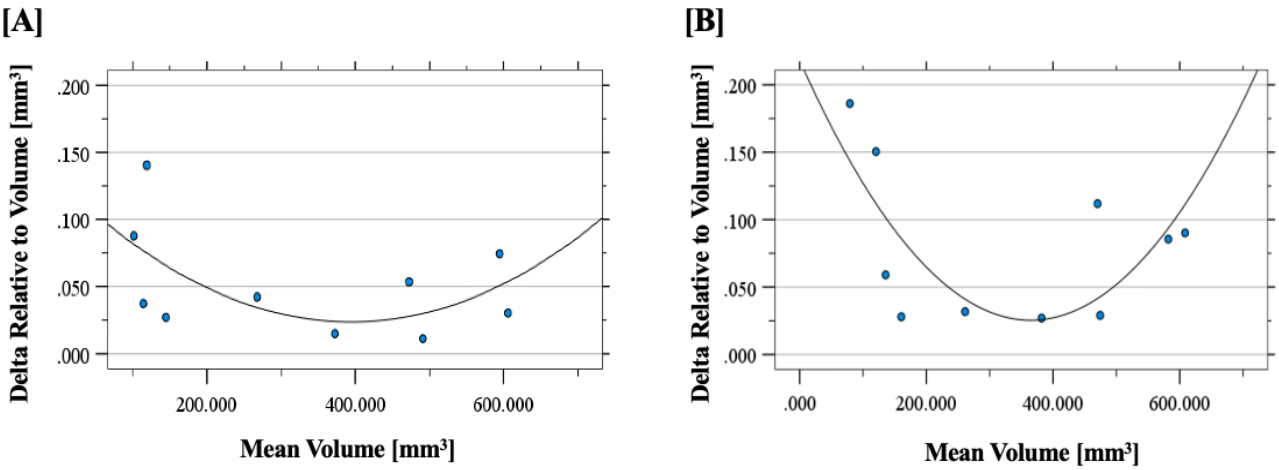

Figure 2.3.3.3: Polynomial regression plots: Polynomial regression plots assessing the relationship between synovial tissue volume and the difference between the repeated volume measurements normalized by the mean volume (i.e., relative delta) for 3D US (A) and MRI (B), respectively.

2.4 Discussion

2.4.1 Linear and Volume System Validation

The linear measurement accuracy using our 3D US images was confirmed using a multilayer microfilament grid phantom, as the largest percentage distance error was 1.06% in the reconstruction plane of the 3D US image. This result is consistent with error measurements found in previous 3D US phantom studies, which reported error values as high as 3.0%.[31,36]

We demonstrated that the system has the ability to accurately measure the volumes of irregular anatomy in a CMC1 phantom with $< 2\%$ error from the known physical volume of the embedded object. In a previous study, Papernick et al. reported a 0.49% error between knee cartilage tissue simulating agar phantom and its known physical volume.[28] The Papernick *et al.* study used the same equipment and linear scanning methods as our study; however, their study aimed to examine the cartilage volume of the knee, and as such, the volume phantom used for their study consisted of a larger-regular shaped object which was less challenging to manually segment. Thus, the larger percent error in the assessment of the synovial volume (1.8%) found in our study was associated with the irregular shape and small size of the CMC1 phantom, which made accurate segmentation more challenging and small segmentation errors causing a larger percentage error.

2.4.2 Clinical Validation

3D US synovial volume segmentations demonstrated insignificant mean differences between raters for the CMC1 synovial volume measurements compared to MRI. The percent difference between 3D US and MRI was 1.71%. Manually segmenting the synovial tissue on non-contrast MRI was challenging as the effusion boundaries are not always as well defined as observed in our 3D US images. Movement artifact is often easier to overcome in 3D US as we

are able to re-acquire images rapidly if needed. However, with MRI, acquiring sequences takes time and requires the patient to stay still for long periods of time (30 minutes), often in uncomfortable positions. Additionally, there was a difference in slice thickness between the MRI and 3D US images. The 2D images that comprised the 3D US reconstruction were spaced 0.33mm apart, while the MRI slice thickness was 0.5mm. An increase in slice thickness causes a decrease in resolution, which could possibly have constributed to the quality of the images and the accuracy of the segmentations. However, Papernick *et al.* used similar methods to examine healthy knee tibiofemoral cartilage thickness and found a percent difference of 6.46% between volume measurements found using MRI versus 3-D US.[25] Healthy knee cartilage is more uniform and consistent than the synovial tissue membrane of the CMC1 joint. The knee joint is also much larger and is easier to visualize using ultrasound as the joint consists of larger articulating bones and is easily opened for view by bending the knee. In the hand, visualizing the joints is typically more challenging due to the small size, irregular shape, and biomechanical limitations of the structures. However, the anatomical shape and small size of the CMC1 joint often leads to distinct protrusion of the synovial fluid on the volar side of the joint, which makes identification and segmentation easier. This could explain why we found a smaller percent difference between our MRI and 3D US values (1.78%) compared to the 6.46% difference in femoral articular cartilage volumes reported by Papernick *et al.*

The inter- and intra-rater reliability assessment demonstrated excellent reliability for both 3D US (ICC = 0.94) and MRI (ICC=0.99) based on the Intra-Correlation Coeffient criteria previously outlined in this chapter. The SEM for our 3D US volume measurements (11.21 mm^3) was smaller than the values found for MRI (16.82 mm^3), indicating that there was a higher level of precision associated with the 3D US measurements than with MRI. The smaller MDC value

for 3D US compared to MRI suggests that our 3D US imaging device is more sensitive to detecting differences in repeated synovial tissue volume segmentations than MRI. The DSC (88.0%) and HD (0.34 ± 0.17 mm) values found for the volumetric phantom were similar to values found in the clinical populations of other studies conducted using MRI for automatic and semi-automatic segmentations of knee bone and cartilage [28,37]. Fripp J *et al*., reported DSC values of 87.0%, 85.0%, and 87.0% for patellar, tibial, and femoral cartilage MRI volume segmentations, respectively[37]. These results suggest that the application of this 3D US device to a longitudinal or test-retest study design would allow for an examination of the device's ability to detect the MDC between patient images. This exploration would provide information on synovial volume changes over time and give clinicians insight into which magnitude of change should be considered significant. Once these values have been established, 3D US may be suggested to measure effects in a clinical trial and in monitoring an individual's progression of synovitis in CMC1 OA patients would be better than with the use of MRI.

2.4.4 Limitations

While 3D US is an imaging modality with many advantages, such as its non-invasive, point-of-care nature, and quantitative measurement capabilities, there are inherent limitations. Potential sources of error within our study lie within the positioning of patients, MRI sequences, and the post-acquisition process. For the CMC1 population, patients were imaged using 2D and 3D US in two main positions, dorsal and volar (palmer), scanning through the thenar eminence. The CMC1 joint is a saddle-shaped joint, forcing the image to be acquired in positions that allow for views into the joint space and to assess joint health.

Disease-specific factors also affected our ability to measure synovial tissue volume in the joint while using 3D US. In CMC1 OA patients, specifically those that are at more advanced

stages of the disease, it is very likely that views of the synovial membrane will be obstructed by abnormal changes to the skeletal anatomy, such as the development of marginal osteophytes and subluxation of the joint (common features in OA). Unlike MRI, high-frequency US is not able to penetrate cortical bone, which results in obscuring underlying synovitis in the 3D US images. Subluxation of the joint and significant functional disability also causes issues with positioning the hand and wrist within the scanning apparatus, which can have deleterious effects on image quality. In the future, these barriers may be partially overcome by acquiring multiple 3D US images of the joint from varying perspectives/angulations of the US transducer and fusing these acquisitions. This approach is a similar concept to compound imaging in that multiple scans of a region of interest from different view angles can overcome the limitations of obfuscated anatomy and imaging artefacts[38].

In addition to the limitations associated with physical hand position and disease-specific factors in imaging, consistency in hand positioning over time and between modalities scans was another limitation. To accurately compare and assess synovitis using our 3D US device, we must position patients in the same position each time we acquire the images. This process must be executed when transferring patients from the 3D US device to the MRI machine. Variation in position could influence the volumetric quantity and shape of synovitis and synovial membrane observed from the 3D US images, which would result in variation in the observed synovial tissue volume. Although our hand positioning device did mitigate some of the positioning variations, there was inevitable compression of the joints due to the MRI coil requirements.

2.5 Impact

The most significant advantage of 3D US is the ability to acquire images safely, quickly, and efficiently at the patient's bedside. The small SEM and MDC values indicate that 3D US can detect small changes in synovial tissue volume measurements with more precision and sensitivity than MRI. This indicates that 3D US may be an effective tool to consider when investigating characteristics of CMC1 OA in longitudinal and test-retest study designs. It also provides a cost-effective and non-invasive method for assessing and monitoring synovial tissue status earlier in the HOA disease process. The simple operation requirements and non-operator dependent nature of the device provide clinicians a point-of-care method for use in clinics and practices. With the availability of quantitative imaging methods, clinicians will have the tools to potentially screen and monitor HOA earlier than the clinical standard today, leading to earlier and inherently less invasive treatment options for patients. Future work will assess how the synovial membrane and levels of synovitis respond to disease progression over time and what impact treatment options such as intra-articular joint injections potentially have on synovial tissue volume. In Chapter 3 of this thesis, we aim to evaluate the relationship between patient-related outcomes, 3D US acquired synovial tissue volume, and the morphological presentation of CMC1 OA on various medical imaging modalities in a larger cohort of patients with CMC1 OA.

Three-dimensional ultrasound shows promise as a tool for quantitatively characterizing and monitoring synovial tissue volume in the hands and wrists. The study results provide the basis to show that 3D US can accurately measure synovial tissue volume in patient populations. We have demonstrated that 3D US segmentations of volumetric and linear phantoms were associated with low acquisition error when compared to known physical volumes. Notably, the low SEM and

MDC values make the detection of small changes in synovial tissue volume measurements possible when monitoring synovitis in various upper limb OA patients.

2.6 References

[1] Kloppenburg M, Kwok WY. Hand osteoarthritis—a heterogeneous disorder. *Nature Reviews Rheumatology.* 2012*;* 8, 22–31. https://doi.org/10.1038/nrrheum.2011.170

[2] Sharif B, Kopec J, Bansback N, et al. Projecting the direct cost burden of osteoarthritis in Canada using a microsimulation model. *Osteoarthritis and Cartilage*. 2015; 23(10): 1654-1663. https://doi.org/10.1016/j.joca.2015.05.029.

[3] Centers for Disease Control and Prevention (CDC). A National Public Health Agenda For: Osteoarthritis: 2020 Update 2020. https://www.cdc.gov/arthritis/docs/oaagenda2020.pdf

[4] Klippel JH, Weijand CM, Wortmann RL, Hochberg MC. Osteoarthritis – clinical features and treatment. In: Klippel JH, Weijand CM, Wortmann RL, eds. *Primer on the rheumatic diseases*. 11th ed. Atlanta: Arthritis Foundation, 1997:218.

[5] Li, W. Carpometacarpal osteoarthritis of the thumb. *Canadian Medical Association Journal. 2013; 185*(2), 149–149. https://doi.org/10.1503/cmaj.111444

[6]Haugen IK, Englund M, Aliabadi P, et al. Prevalence, incidence, and progression of hand osteoarthritis in the general population: the Framingham Osteoarthritis Study. *Annals of the rheumatic diseases*. 2011; *70*(9), 1581–1586. https://doi.org/10.1136/ard.2011.150078

[7]Kodama R, Muraki S, Oka H, et al. Prevalence of hand osteoarthritis and its relationship to hand pain and grip strength in Japan: The third survey of the ROAD study. *Modern Rheumatology*.2016; *26*(5), 767–773. https://doi.org/10.3109/14397595.2015.1130673

[8] Dahaghin S, Bierma-Zeinstra SM, Ginai AZ, et al. Prevalence and pattern of radiographic hand osteoarthritis and association with pain and disability (the Rotterdam study). *Annals of the rheumatic diseases*.2005; *64*(5), 682–687. http://dx.doi.org/10.1136/ard.2004.023564

[9] Haugen IK, Bøyesen P. Imaging modalities in hand osteoarthritis--and perspectives of conventional radiography, magnetic resonance imaging, and ultrasonography. *Arthritis research & therapy*. 2011; *13*(6), 248. https://doi.org/10.1186/ar3509

[10]Scanzello C, Goldring S. The role of synovitis in osteoarthritis pathogenesis. *Bone.* 2013; 51(2), 249–257. https://doi.org/10.1016/j.bone.2012.02.012

[11] Maheu E, Altman RD, Bloch DA, et al. Design and conduct of clinical trials in patients with osteoarthritis of the hand: recommendations from a task force of the Osteoarthritis Research Society International. *Osteoarthritis Cartilage.* 2006; 14, 303–322. doi: 10.1016/j.joca.2006.02.010

[12] Dahaghin S,Bierma-Zeinstra SM, Hazes JM, *et al*. Clinical burden of radiographic hand osteoarthritis: a systematic appraisal. *Arthritis Rheum. 2006*; 55, 636–47.

[13] de Vries BA, Breda SJ, Sveinsson B, et al. Detection of knee synovitis using non-contrast-enhanced qDESS compared with contrast-enhanced MRI. *Arthritis Res Ther*. 2021; 23(1):55. doi:10.1186/s13075-021-02436-8

[14] Wenham CY, Conaghan PG. The role of synovitis in osteoarthritis. *Ther Adv Musculoskelet Dis*. 2010;2(6):349-359. doi:10.1177/1759720X10378373

[15] Oo, D. Musculoskeletal ultrasound in symptomatic thumb-base osteoarthritis: clinical, functional, radiological and muscle strength associations. *BMC Musculoskeletal Disorders*. 2019; *20*(1): 220–220. https://doi.org/10.1186/s12891-019-2610-4

[16]Mathiessen A, Conaghan PG. Synovitis in osteoarthritis: current understanding with therapeutic implications. *Arthritis research & therapy*. 2017; *19*(1): 18. https://doi.org/10.1186/s13075-017-1229-9

[17]Hayashi D, Roemer FW, Katur A et al. Imaging of Synovitis in Osteoarthritis: Current Status and Outlook. *Seminars in Arthritis and Rheumatism*. 2011; 41 (2): 116-130. https://doi.org/10.1016/j.semarthrit.2010.12.003.

[18]Xiao H, Liu M, Tan L, et al. Value of ultrasonography for diagnosis of synovitis associated with rheumatoid arthritis. *International Journal of Rheumatic Diseases*. 2014; *17*(7): 767–775. https://doi.org/10.1111/1756-185X.12390

[19]Keen H, Wakefield R, Grainger A, et al. An ultrasonographic study of osteoarthritis of the hand: Synovitis and its relationship to structural pathology and symptoms. *Arthritis and Rheumatism*. 2008; *59*(12): 1756–1763. https://doi.org/10.1002/art.24312

[20] Fenster A, Downey DB, Cardinal HN. Three-dimensional ultrasound imaging. *Physics in Medicine and Biology.* 2001; 46(5):67–99. https://doi.org/10.1088/0031-9155/46/5/201

[21]Hyun CK, Sang WK, Dal MY. What are the Benefits of The Matrix Array Transducer in 2D And 3D Ultrasonographic Imaging of The Abdomen? *Ultrasound in Medicine & Biology.* 2015; 41(4):131. https://doi.org/10.1016/j.ultrasmedbio.2014.12.515.

[22]Clendenen SR, Robards CB, Clendenen NJ, Freidenstein JE, Greengrass RA. Real-time 3-dimensional ultrasound-assisted infraclavicular brachial plexus catheter placement: implications of a new technology. Anesthesiol Res Pract. 2010. doi:10.1155/2010/208025.

[23]Smith SW, Trahey GE, von Ramm OT. Two-dimensional arrays for medical ultrasound. *Ultrasonic Imaging*. 1992;14(3):213-233. https://doi.org/10.1016/0161-7346(92)90064-3

[25]Egger M, Krasinski A, Rutt B, et al. Comparison of B-Mode Ultrasound, 3-Dimensional Ultrasound, and Magnetic Resonance Imaging Measurements of Carotid Atherosclerosis. *Journal of Ultrasound in Medicine*. 2008;*27*(9): 1321–1334. https://doi.org/10.7863/jum.2008.27.9.1321

[26]Cool D, Sherebrin S, Izawa J, et al. In vitro validation of a 3-dimensional transrectal ultrasound system for prostate biopsies. *Clinical and Investigative Medicine*. 2007;*30*(4):77–. https://doi.org/10.25011/cim.v30i4.2846

[27]Kishimoto J, Fenster A, Lee D, de Ribaupierre S. In Vivo Validation of a 3-D Ultrasound System for Imaging the Lateral Ventricles of Neonates. *Ultrasound in Medicine & Biology*. 2016; *42*(4): 971–979. https://doi.org/10.1016/j.ultrasmedbio.2015.11.010

[28]Papernick S, Robert D, Gillies D, Appleton T, Fenster A. Reliability and concurrent validity of three-dimensional ultrasound for quantifying knee cartilage volume. Osteoarthritis and Cartilage Open. 2020; 2(4). https://doi.org/10.1016/j.ocarto.2020.100127

[29] Budorick NE, Pretorius DH, Johnson DD, Tartar MK, Lou KV, Nelson TR. Three-dimensional ultrasound examination of the fetal hands: normal and abnormal. *Ultrasound in Obstetrics and Gynecology*. 1998;12(4):227-234. doi:10.1046/j.1469-0705.1998.12040227.x.

[30] Yanping H, Choi HC, Guangquan Z, Yongping Z, Chun HY, Chunyi W. 3D High-Frequency Ultrasound Imaging of Cartilage-Bone Interface Compared with Micro-CT. *BioMed Research International*. 2020; 2020. https://doi.org/10.1155/2020/6906148

[31] Papernick S, Gillies DJ, Appleton T, Fenster A. Three-dimensional ultrasound for monitoring knee inflammation and cartilage damage in osteoarthritis and rheumatoid arthritis. *Proc. SPIE 11315, Medical Imaging 2020: Image-Guided Procedures, Robotic Interventions, and Modeling*. 2021. https://doi.org/10.1117/12.2549624

[32] Chauvin NA, Doria AS. Ultrasound imaging of synovial inflammation in juvenile idiopathic arthritis. *Pediatr Radiol*. 2017 ;47(9):1160-1170. doi: 10.1007/s00247-017-3934-6. Epub 2017 Aug 4. PMID: 28779188.

[33] Lai K, Chen D, Chen Y, Huang W, Hsieh T, Hsieh C, Chen Y, Hung W, Chen H. Assessment of wrist joint inflammation in patients with rheumatoid arthritis by quantitative two- and three-dimensional power Doppler ultrasonography. *Clinical and Experimental Rheumatology*. 2014; *32*(5): 674–679.

[34]Beaton DE, Bombardier C, Katz JN, Wright JG. A taxonomy for responsiveness. *Journal of Clinical Epidemiology.* 2001; 54 (12): 1204-1217. https//doi.org/10.1016/S0895-4356(01)00407-3

[35] Koo TK, Li MY. A guideline of selecting and reporting intraclass correlation coefficients for reliability research. *J Chiropr Med*. 2016; 15 (2): 155–163. https:// doi.org/10.1016/j.jcm.2016.02.012.

[36]Rodgers JR. Development and Validation of Tools for Improving Intraoperative Implant Assessment with Ultrasound during Gynaecological Brachytherapy. *Electronic Thesis and Dissertation Repository*. 2020; 7481.

[37] Fripp J, Crozier S, Warfield SK, Ourselin S. Automatic Segmentation of Articular Cartilage in Magnetic Resonance Images of the Knee. In: Ayache N, Ourselin S, Maeder A, eds. *Medical Image Computing and Computer-Assisted Intervention – MICCAI 2007*. Vol 4792. Lecture Notes in Computer Science. Springer Berlin Heidelberg; 2007:186-194. doi:10.1007/978-3-540-75759-7_23

[38] Entrekin RR, Porter BA, Sillesen HH, Wong AD, Cooperberg PL, Fix CH. Real-time spatial compound imaging: application to breast, vascular, and musculoskeletal ultrasound. *Semin Ultrasound CT MR*. 2001;22(1):50-64. doi:10.1016/s0887-2171(01)90018-6

Chapter 3

3 Evaluation of Three-Dimensional Ultrasound as a Tool to Examine Synovitis Volume and Morphology in Relation to Patient Reported Outcomes

3D US imaging has the potential to improve the efficiency of clinical workflow and to assist in monitoring disease progression and treatment efficiency in CMC1 OA patients. The purpose of Chapter 3 is to present the observed morphological trends in synovitis and examine its relationship with patient-reported outcomes of pain and functional disability.

3.1 Introduction

The thumb is critical to hand function, being responsible for precision movements and grip, and plays a significant part in nearly all basic activities of daily living[1]. As stated in Chapter 1, the biconcave-convex structure of the CMC1 joint and its reliance on muscular and ligamentous stabilization increases its susceptibility to osteoarthritis[2]. Studies have shown that over 30% of middle-aged women (fifty years of age) have arthritis in their CMC1 joint[3]. CMC1 OA is commonly diagnosed clinically with the aid of x-ray radiography. X-ray serves its primary purpose as a diagnostic imaging tool; however, it is also used to estimate prognosis, guide treatments, and for post-therapeutic evaluation. Therapeutic treatment options, such as surgery, are considered using the presence and extent of radiographic abnormalities[4]. The two most common radiographic indicators of OA are joint space width and the Eaton-Littler scoring system. This system has been deemed the gold standard for assessing osteoarthritis and ranges from 0 to 4, with grade 0 = no features of joint changes and grade 4 = joint space greatly impaired with sclerosis of the subchondral bone[5,6]. However, studies have reported discrepancies between radiographic evidence of OA and patient-reported outcomes such as pain and

disability[4,7,8]. If we look at the osteoarthritis literature, we can see that most patients with pain do not exhibit radiographic changes associated with OA and that less than 50% of individuals who have radiographic evidence of OA report pain regardless of the area affected[9,10,11,12]. These discrepancies have been attributed to the lack of soft-tissue contrast associated with radiography and the heterogeneous nature of osteoarthritis as a disease.

Synovitis has been associated with pain and disability and has been proven to be a driver of osteoarthritis disease progression, making it an attractive target for disease-modifying interventions[13,14,15,16] . Non-contrast MRI and 2D US are commonly used tools for assessing synovitis in OA patients. Studies examining synovitis and pain in knee OA patients demonstrate that synovitis was present in 55% of patients with no radiographic evidence of OA. The Multicenter Osteoarthritis Study (MOST) showed that 80% of the participants who reported moderate pain had synovitis upon imaging analysis[17]. In 2016, the Outcome Measures in Rheumatoid Arthritis Clinical Trials Ultrasound group developed definitions and semi-quantitative grading schemes for synovitis, and subsequent studies have established moderate linear relationships between patient-reported outcome scales such as the Knee Osteoarthritis Outcome Score and OMERACT grading scores[18]. However, studies investigating the relationship between synovitis (synovial effusion and membrane hypertrophy) and various grading scales and patient outcomes have found conflicting results. Hall et al. found that although US abnormalities are common in OA, there is only a moderate correlation between synovial effusion and hypertrophy and radiographic severity. Additionally, the results indicated that the relationship between these imaging features and pain is weak[19]. In contrast, Naredo et al. found that only those with symptomatic OA had joint effusion, meniscal protrusion, and bulging

of surrounding ligaments. They demonstrated an increased risk for developing painful OA when effusion is present[20].

We believe these discrepancies may be attributed to variable definitions of inflammatory features, a lack of sensitive quantitative measures for synovitis, and the possibility of variation in pathophysiological contributors within potential CMC1 OA phenotypes. Therefore the objectives of our study are:

1. To examine sonographic features associated with CMC1 OA in a cohort of patients. Sonographic features include synovial tissue volume as well as effusion morphology.
2. To determine if synovial tissue volume is a predictor of patient-reported arthritic pain.

3.2 Methods

3.2.1 Participants

Nineteen CMC1 OA patients over the age of 18 were recruited by an experienced hand surgeon or rheumatologist at the Roth|McFarlane Hand and Upper Limb Center. In addition, five volunteers over the age of 18 without prior history of chronic CMC1 joint pathology were also recruited. The study protocol was approved by the Research Ethics Board at Western University, Canada, and all participants provided written consent prior to participating in the study (Appendix A). Patients were diagnosed with CMC1 OA by a fellowship-trained hand surgeon or a rheumatologist based on clinical indicators and radiography studies. Volunteers were deemed healthy if they denied experiencing any prior CMC1 pain or injury to the area. Patients with CMC1 OA who were scheduled to receive long-acting corticosteroid injections or had received an injection within a three-month period were scheduled to join our study only after the three-

month drug activation period had passed as corticosteroid drugs influence the volume of synovitis present in the joint, as well as patient-reported symptoms such as pain and disability[66].

3.2.2 3D US Image Acquisition

3D US scans were acquired using an Aplio i800 US machine (Canon Medical Systems Corporation, Otawara, Tochigi, Japan) and a 14L-5 linear transducer. The transducer has an operating frequency of 10 MHz (3.8 MHz – 10.0 MHz) and a 58 mm footprint length. The 2D US transducer was connected to our 3D US device using a custom 3D- printed mold. Our 3D US device consisted of a semi-submerged motorized drive mechanism that linearly translated the 2D transducer over a 7.9 cm length above the patient's submerged thumb. Images were acquired continually at regular spatial intervals. These 319 2D US images were then reconstructed into a 3D image in real-time while the scan was conducted via computer software created by Dr. Fenster's lab. This scanner was previously validated in 10 CMC1 OA patients and compared to MRI as described in Chapter 2.

3.2.3 2D US Scanning

In addition to the 3D US images, 2D US images were acquired and graded using the Outcome Measures in Rheumatology (OMERACT) (2D US) semi-quantitative grading scales. The EULAR- OMERACT grading was based on the grading definitions reported by D'Agostino et al.[21,22]. Grade 1 is classified as the absence of hypoechoic synovial hypertrophy, regardless of the presence of effusion, and without Power-Doppler signal detected in the synovium. Grade 2 is defined as the grey-scale synovitis is hypertrophic regardless of the presence of effusion and any grade of Power Doppler signal. Grade 3 is indicated as a positive Power- Doppler signal that equals at least one red spot within the hypoechoic synovial hypertrophic region.

The Eaton-Littler grading was completed by our team's hand surgeon, who assessed and graded the images using the grading definitions outlined by Eaton and Glickel[23,24]. The Eaton-Littler classification system describes the four stages of CMC1 arthrosis. This is based on lateral radiographs of the CMC1 joint and includes the sesamoid bones superimposed on one another. Stage 1 shows normal radiographs with the absence of joint space narrowing, cyst formation, or subchondral bone changes. This stage may have joint space widening attributed to synovitis, effusion, or laxity of the surrounding ligamentous structures of the joint. In contrast, stage 2 features slight joint-space narrowing, sclerosis, and cystic changes with the presence of osteophytes smaller than 2 mm in diameter. Stage 3 includes advanced joint space narrowing, sclerosis, and cystic changes with osteophytes larger than 2 mm in diameter, and stage 4 includes all aspects of stage 3 but extends to scaphotrapezial arthritis.

3.2.4 Patient-Reported Outcomes

The primary outcome measure in this study was pain and disability, quantified using the Australian Canadian Hand Osteoarthritis Index (AUSCAN). The AUSCAN questionnaire is a self-administered pain interference scale that assesses the dimensions of pain, disability, and joint stiffness in hand osteoarthritis using fifteen questions. The fifteen questions assessing pain and disability were scaled on a 100 mm Visual Analog scale, where one end of the line represented no pain, and the other represented the worst possible pain ever experienced. Patients were asked to fill out the questionnaire while thinking about how their CMC1 joint felt on the day of the appointment. The two-point pinch grip test was conducted by one researcher using a Jamar pinch gauge dynamometer (0-45 pounds) (Patterson Medical Holdings Inc., Greensboro, North Carolina, US). Participants were instructed to apply force to the dynamometer until they started to feel pain and slowly release the device to try and mitigate further exacerbation of pain

potentially caused by a quick-release motion. Three trials were completed on each hand, and the mean force was calculated and recorded.

3.2.5 Analysis

A descriptive analysis was used to describe how synovial tissue volume changes in morphology and pathology as the grade of radiographic findings differs, how these changes are related to outcomes of pain and functional strength, and the role of 3D US analysis in defining these. The second aim of this study was to determine if synovial tissue volume is a predictor of patient-reported arthritic pain, stiffness, and disability. Therefore, a forward stepwise linear regression was conducted to investigate the association between OMERACT grade, Eaton-Littler grade, pinch grip force (predictor variables) and AUSCAN score (dependent variable). Each independent variable was added to the model separately. After each entry, all candidate variables were checked to assess if their significance has been reduced below the specified significance level. Predictor variables were retained if the change in the p-value for additional variance explained was less than 0.05 when each entry was made.

3.3 Results

Table 3.3.2 shows a summary of the characteristics of the healthy participant cohort. The mean age for the healthy volunteer group was 38.3 years, and 60% of the volunteers were female. The average OMERACT score was 0.2, and the mean synovial tissue volume was 35.4 mm^3 for the healthy cohort. The healthy volunteers reported an average AUSCAN score and pinch grip force of 1.2% and 19.4 KgF, respectively.

Table 3.3.1 shows the patient demographics of the 19 participants enrolled in this study. The mean age of the patient group was 66.1 (SD = 6.5) years, and 63% of the patients were female. The mean Eaton-Littler grade was 2.8 (SD = 0.6), while the mean OMERACT score was

2.1 (SD = 0.8). The average synovial tissue volume found using 3D US was 243.63 mm^3 (SD = 200.2), while patients reported an average AUSCAN score of 50.7% (SD = 23.9) and a mean pinch grip force of 10.6 KgF. The stepwise linear regression reported that pinch grip force predicted 28.4% of the variability in the AUSCAN scores (adjusted R^2 value 0.284) ($p<0.001$) (Table. 3.3.1). Synovial tissue volume, OMERACT score, and Eaton-Littler grade did not significantly increase the variance explained within the model and were not retained.

Table 3.3.1: Model summary of patient characteristics and differences between AUSCAN scores.

Model	R	R Square	Adjusted R Square	Std. Error of the Estimate
1	0.576	0.332	0.284	0.846278

Predictors: (Constant), Zscore Pinch Grip

Table 3.3.2: Summary of demographic characteristics for healthy volunteers.

	Healthy Participants
Sex (% Female)	60%
Age ± SD	38.3 ± 16.0
Average	
OMERACT Score	0.2 ± 0.4
Synovial Tissue Volume (mm^3)	35.4 ± 24.9
AUSCAN (%)	1.2 ± 2.2
Pinch Grip (KgF)	19.4 ± 9.9

ID	2DUS	3DUS	3DUS (mm^3)	Sex/Age	Pinch Grip (KgF)
011	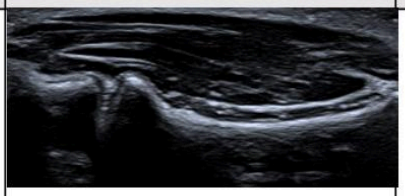 OMERACT: 0	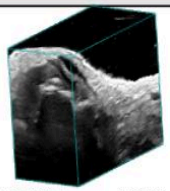 STV Volume: 16.58	1.0	F/26	16.4
012	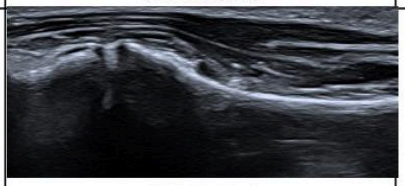 OMERACT: 0	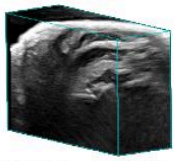 STV Volume: 20.36	0	F/21	14
013	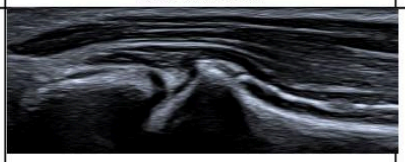 OMERACT: 0	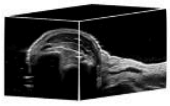 STV Volume: 17.14	0	M/34	21.3
043	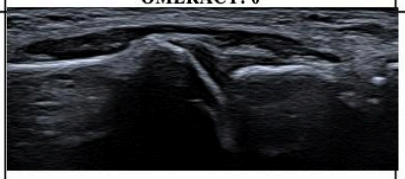 OMERACT: 1	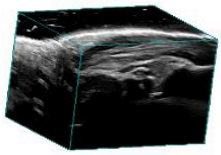 STV Volume: 72.10	5.0	F/55	10
044	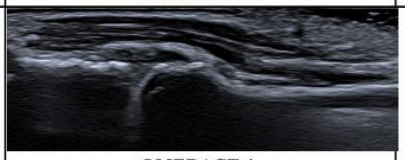 OMERACT:1	 STV Volume: 50.79	0	M/55	35.3

Figure 3.3.1: Healthy Participants Summary. A chart demonstrating the imaging features, clinical, and demographic characteristics of healthy CMC1 participants. The healthy synovium in the 2D US shows a classical pattern of closely forming around the joint with almost no visible anechoic sonographic features between the bones.

Within our patient population, we observed three distinct morphological presentations of synovitis:

Phenotype 1: **Synovial Effusion Dominant**

Phenotype 2: **Diffuse Synovial Effusion and Hypertrophy**

Phenotype 3: **Osteochondral Dominant**

These phenotypes were distinguished by synovial tissue margin properties, synovial tissue volume, and pathophysiological (effusion vs. hypertrophy). Table 3.3.3 summarizes the mean imaging grades, synovial tissue volume, demographics, AUSCAN scores and pinch grip strength for each phenotype.

Table 3.3.3: Patient demographics summary for each synovial tissue phenotype.

	Synovial Effusion Dominant	**Diffuse Synovial Effusion and Hypertrophy**	**Osteochondral Dominant**
Sex (% Female)	20%	71%	100%
Age ± SD	63.6 ± 7.1	65. 43 ± 6.1	70.5 ± 4.0
Averages			
Eaton-Littler Score	2.6 ± 0.5	2.6 ± 0.5	3.5 ± 0.5
OMERACT Score	2.8 ± 0.4	2.1 ± 0.6	1.8 ± 0.8
Synovial Tissue Volume (mm^3)	436.8 ± 195.8	287.7 ± 133.4	29.4 ± 18.2
AUSCAN (%)	49.6 ± 28.5	36.6 ± 21.3	69.3 ± 5.7
Pinch Grip (KgF)	11.84 ± 5.5	13.1 ± 4.2	8.33 ± 2.3

3.3.1 Phenotype 1: ***Synovial Effusion Dominant***

The first morphology is described as concave extrusion of the synovial fluid, and in some cases, synovial hypertrophy was observed in addition to this presentation. Fig. 1 shows the radiographs, 2D US, 3D US, AUSCAN score, pinch grip strength, sex, and age of each patients allocated to the synovial effusion dominant phenotype group. Patients with this morphology had moderate volumes of synovitis compared to the other two groups and tended to have more anechoic signal present in the ultrasound images. These patients also demonstrated mild to moderate synovial membrane hypertrophy as indicated by regions of hypoechoic tissue surrounding the joint. Compared to the other two phenotypes observed, these patients had the lowest average amount of pain interference as indicated by the AUSCAN scores and the highest physical function measured by the pinch grip test.

Eaton-Littler grades for radiographic evidence of OA were typically classified as stage 2 and 3 for this sub-group and stayed consistent between subgroups with the exception of the low-synovitis, high osteochondral involvement phenotype, which includes two patients with stage 4 radiographic evidence of OA.

ID	X-ray	2DUS	3DUS (mm^3)	AUSCAN (%)	Sex/Age	Pinch Grip (KgF)
002	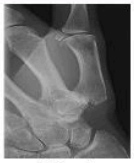 EL: 3	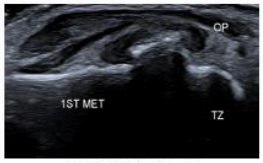 OMERACT: 3	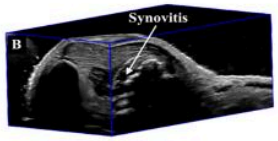 STV Volume: 375.4	53%	M/59	15.0
007	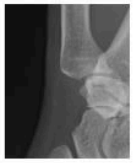 EL: 2	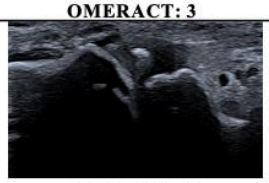 OMERACT: 3	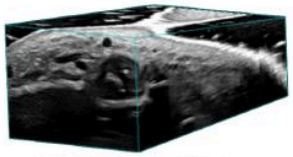 STV Volume: 572.6	61%	M/60	16.3
016	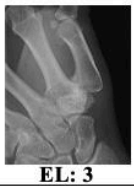 EL: 3	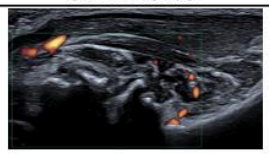 OMERACT: 3	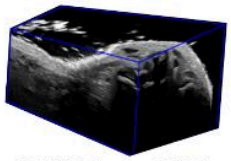 STV Volume: 615.2	66%	M/76	6.3
019	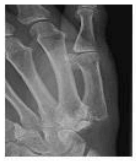 EL: 3	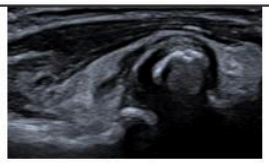 OMERACT: 3	 STV Volume: 126.8	0%	F/60	16.3
039	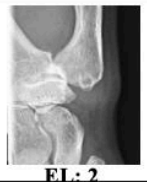 EL: 2	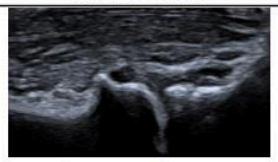 OMERACT: 3	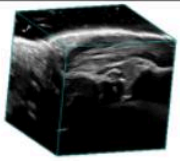 STV Volume:493.9	69%	M/63	5.3

Figure 1 Phenotype 1: Synovial Effusion Dominant. A chart demonstrating the imaging features, clinical and demographic characteristics of patients allocated to the synovial effusion dominant phenotype.

Phenotype 2 ***Diffuse Synovial Effusion and Hypertrophy***

The second presentation is described as diffused synovial effusion and hypertrophy that spreads out of the joint line and over the proximal end of the trapezium and towards the distal end of the first metacarpal (Fig.2). Patients in this sub-group presented with the highest synovial tissue volumes and a moderate amount of pain interference in comparison to the other two sub-groups. These patients presented with predominantly areas of hypoechoic signal, indicating that the tissue is primarily composed of hypertrophic synovial membrane instead of fluid effusion.

An increased presence of osteophytes was also observed in the images of patients allocated to this group. Functionally, these patients performed worse on the pinch grip test than those in the effusion dominant group, as indicated by lower average pinch grip forces.

ID	X-ray	2DUS	3DUS (mm^3)	AUSCAN (%)	Sex/Age	Pinch Grip (KgF)
008	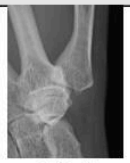 EL: 2	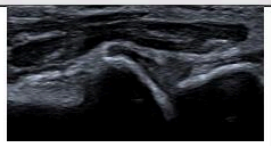 OMERACT: 2	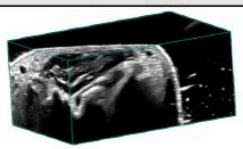 STV Volume: 111.88	13%	M/54	19.3
010	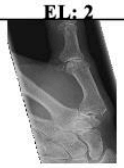 EL: 3	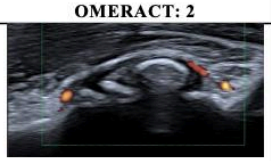 OMERACT: 3	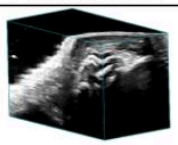 STV Volume: 368.86	12%	F/66	10.0
021	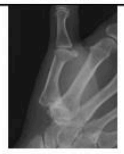 EL: 3	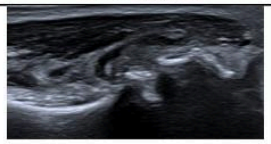 OMERACT: 3	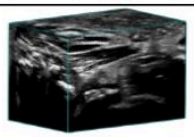 STV Volume: 485.14	63%	F/75	6.5
023	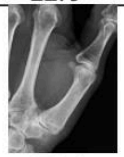 EL: 3	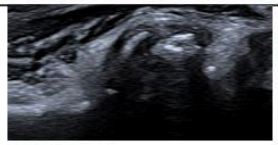 OMERACT: 3	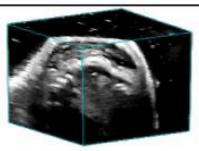 STV Volume: 203.58	42%	F/63	16.0
035	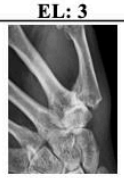 EL: 3	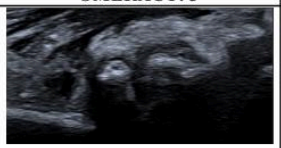 OMERACT: 3	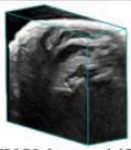 STV Volume: 142.92	17%	M/71	16.7
037	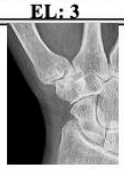 EL: 2	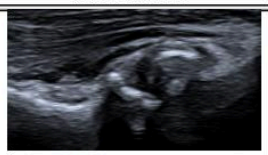 OMERACT: 2	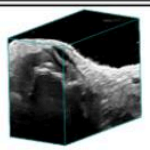 STV Volume: 428.66	43%	F/65	10
038	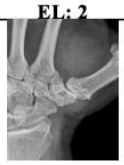 EL: 2	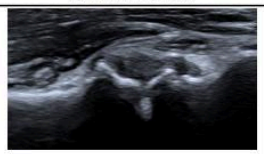 OMERACT: 2	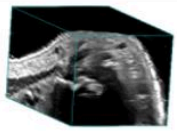 STV Volume: 273.19	66%	F/64	13.7

Figure 2 Phenotype 2: Diffuse Synovial Effusion and Hypertrophy. A chart demonstrating the imaging features, clinical and demographic characteristics of patients allocated to the diffuse synovial effusion and hypertrophy phenotype.

Phenotype 3: ***Osteochondral Dominant***

The final presentation observed were the patients with very little synovitis and synovial hypertrophy but advanced osteophyte growth and joint space narrowing. Two of the four patients with this morphology were assigned an Eaton-Littler grade of 4/4, indicating that they had decreased trapeziometacarpal joint space narrowing, subchondral sclerosis, osteophytes, trapeziometacarpal joint subluxation, and involvement of the scaphotrapezial joint. On our 3D US images we observed minimal anechoic and hypoechoic signals indicating low amounts of synovial fluid with minimal amounts of synovial membrane hypertrophy. These patients on average had the highest pain interference ratings on the AUSCAN scale and the lowest average pinch grip strength. Figure 3 highlights a case study from this subgroup.

ID	X-ray	2DUS	3DUS (mm^3)	AUSCAN (%)	SEX/Age	Pinch Grip KgF
014	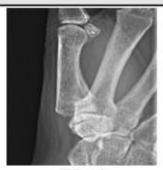 EL: 3	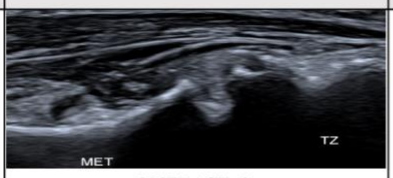 OMERACT: 2	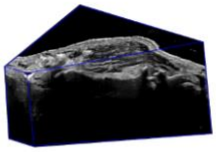 STV Volume: 0.0	77	F/77	11.7
015	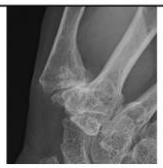 EL: 3	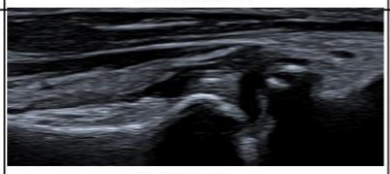 OMERACT: 3	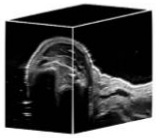 STV Volume: 48.75	66	F/66	9
026	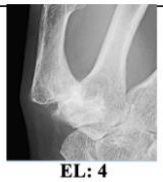 EL: 4	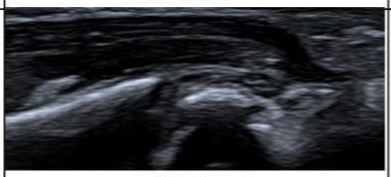 OMERACT: 1	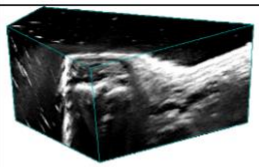 STV Volume: 38.45	62	F/69	7.3
028	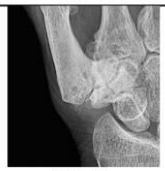 EL: 4	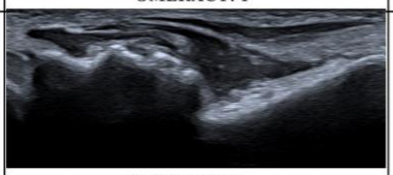 OMERACT: 1	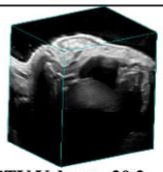 STV Volume: 30.2	72	F/70	5.3

Figure 3 Phenotype 3: Osteochondral Dominant. A chart demonstrating the imaging features, clinical and demographic characteristics of patients allocated to the osteochondral dominant phenotype.

3.4 Discussion

What Information Can Be Gained from Assessing 3D US CMC1 OA Patient Effusion Morphology that Enhances Our Understanding of OA?

This study investigated the clinical application of 3D US acquired synovial tissue volumes as a new marker for OA progression in the CMC1 joint. Our results indicate that three fundamental phenotypes can be seen at varying stages of OA. These phenotypes are distinguished by:

1. Synovial tissue margin properties
2. Synovial tissue volume
3. Histological features (effusion vs. hypertrophy)

The morphological differences between signs of synovitis indicate that the relationship between disease progression, patient-related outcomes, and image-based evidence of OA in the CMC1 joint is complex. The structures involved change not only as we progress to more severe stages of disease, as indicated by radiographs, but also between bouts of inflammation (flare-ups) and between patients. We have observed that the individuals in our study who have moderate synovial tissue volumes comprised predominately of synovial effusion have the lowest average pain interference scores and highest functional scores. We have also observed that these patients predominantly present with uniform concave morphology of their joint effusion. In comparison, our second sub-group of patients presented with more diffuse effusion morphology with increased hypertrophic tissue. These patients also had increased pain interference scores and decreased pinch grip values. Our last sub-group had mostly osteochondral pathology with increased osteophyte presentation, decreased joint space, and decreased synovial tissue volumes. The trends observed in this pilot study follow histological trends described in multiple knee OA (KOA) studies[25,26,27]. Ene et al. state that inflammation seems to be the dominant characteristic and driver of disease progression in earlier stages of KOA. They also state that at earlier stages

of inflammation, effusion seems to be localized to the affected chondral areas but then diffuses as there is an increase in fibrosis of the synovial tissue[28]. Wenham et al. agreed with Ene et al. that there is an over-expression of pro-inflammatory mediators in earlier stages of OA compared to later stages[27]. Since most patients with CMC1 OA do not seek medical assistance until symptoms start impacting activities of daily living, we are limited to investigating patients who tend to have had OA for an extended period. This limits our ability to definitively characterize the early stages of OA as we simply do not see these individuals in clinics. However, even if these patients seek medical assistance earlier, primary care clinicians are less likely to seek advanced imaging or consider using advanced imaging techniques in this early stage of their care. Furthermore, musculoskeletal ultrasound (MSK US) techniques are not emphasized in medical school and are a relatively new addition to sonography programs across Canada. In light of the recent interest in MSK US, professional development courses such as the Canadian Rheumatology Ultrasound Society Basic MSK US course are available for clinicians to broaden their knowledge of diagnostic imaging. However, not all clinicians are interested in participating. The patients in our study were all determined to have Eaton Littler stage 2 or higher radiographic findings of OA, indicating more advanced OA as we see varying degrees of osteochondral pathology.

Does an Increase in Synovial Tissue Volume Correlate to Increased Patient-Reported Outcomes?

Our results indicated that there was not a clear linear relationship between synovial tissue volume and patient-reported outcomes on the AUSCAN survey. When completing a stepwise linear regression analysis, we found that pinch grip was the most significant indicator of pain

interference in CMC1 OA patients (R^2= 0.3). This indicates that approximately 70% of the variance in AUSCAN score was not explained by our model. We believe this is due to the nature of osteoarthritis, where pain may be attributed to different pathological involvements at different stages of disease progression. In knee osteoarthritis, patients have exhibited a trend where in earlier stages, as characterized by radiographic features, patients tend to have increased synovial effusion. This effusion then decreases or changes to synovial membrane hypertrophy and eventually leads to the development of abnormal bone growths called osteophytes in later stages of KOA. We believe we are observing the same trends at the CMC1 joint.

The importance of OA in non-weight bearing joints, such as the small joints of the hand, was not truly understood or emphasized until very recently. As such, there is a distinct lack of outcome measures that focus specifically on those joints. The AUSCAN scale used in this study is considered a global hand OA pain assessment and is therefore not directly focused on thumb motion, pain, stiffness and disability. However, as mentioned before, the AUSCAN scale is currently the most appropriate available scale. This may have had an influence on the discrepancy we observed between our ultrasound measures and the patient-related outcomes.

The first limitation of this study is the small sample size. Although this study was calculated to be significantly powered at 17 patients, we believe this population does not provide adequate variation in OA pathology and stages to generalize our findings to a larger population. We also believe that increasing the diversity of our patient population would potentially see more robust relationships between STV and patient-reported outcomes when those patients are allocated into phenotype sub-groups. Our second limitation is that confounding variables such as administration of non-prescription medication and participation in CMC1 joint aggravating activities before assessments were not controlled. These factors could potentially have a

significant impact on patient-reported outcomes and the STV observed in 3D and 2D US. Finally, although we attempted to control for the effect of corticosteroid injections by waiting three months between the injection date and the study baseline assessment, as indicated by the activation period of long-acting corticosteroid drugs, some patients tend to experience symptom relief and decreased synovitis for longer than that time period.

3.5 Conclusion:

In summary, we observed three distinct morphological CMC1 OA imaging phenotypes, classified as (1) effusion dominant, (2) diffuse effusion and synovial hypertrophy, and (3) osteochondral dominant. Three different imaging techniques, demographic data, and patient outcome measures (AUSCAN score and pinch grip force) were used to describe patients allocated to each of these groups. Stratifying our patients into three phenotypes potentially provides insight into how sonographic features could be used as a method to indicate pain and disease progression. These features may be useful to consider when developing cohorts for clinical trials and for understanding what elements to look for when monitoring CMC1 OA in clinics.

3.6 References

1. Dandy DJ. *Essential Orthopaedics and Trauma*. 2nd ed. Churchill Livingstone; 1993.
2. Gillis J, Calder K, Williams J. Review of Thumb Carpometacarpal Arthritis Classification, Treatment and Outcomes. *Canadian Journal of Plastic Surgery*. 2011;19(4):134-138. doi:10.1177/229255031101900409
3. Guermazi A, Roemer FW, Burstein D, Hayashi D. Why radiography should no longer be considered a surrogate outcome measure for longitudinal assessment of cartilage in knee osteoarthritis. *Arthritis Research & Therapy*. 2011;13(6):247. doi:10.1186/ar3488

4. Bedson J, Croft PR. The discordance between clinical and radiographic knee osteoarthritis: A systematic search and summary of the literature. *BMC Musculoskelet Disord*. 2008;9(1):116. doi:10.1186/1471-2474-9-116

5. Eaton RG, Glickel SZ. Trapeziometacarpal osteoarthritis. Staging as a rationale for treatment. *Hand Clin*. 1987;3(4):455-471.

6. Kennedy CD, Manske MC, Huang JI. Classifications in Brief: The Eaton-Littler Classification of Thumb Carpometacarpal Joint Arthrosis. *Clinical Orthopaedics & Related Research*. 2016;474(12):2729-2733. doi:10.1007/s11999-016-4864-6

7. Lawrence JS, Bremner JM, Bier F. Osteo-arthrosis. Prevalence in the population and relationship between symptoms and x-ray changes. *Ann Rheum Dis*. 1966;25(1):1-24.

8. Davis MA, Ettinger WH, Neuhaus JM, Barclay JD, Segal MR. Correlates of knee pain among US adults with and without radiographic knee osteoarthritis. *J Rheumatol*. 1992;19(12):1943-1949.

9. Hannan MT, Felson DT, Pincus T. Analysis of the discordance between radiographic changes and knee pain in osteoarthritis of the knee. *J Rheumatol*. 2000;27(6):1513-1517.

10. Neogi T, Felson D, Niu J, et al. Association between radiographic features of knee osteoarthritis and pain: results from two cohort studies. *BMJ*. 2009;339:b2844. doi:10.1136/bmj.b2844

11. Birrell F, Croft P, Cooper C, Hosie G, Macfarlane G, Silman A. Health impact of pain in the hip region with and without radiographic evidence of osteoarthritis: a study of new attenders to primary care. The PCR Hip Study Group. *Ann Rheum Dis*. 2000;59(11):857-863. doi:10.1136/ard.59.11.857

12. Dahaghin S. Prevalence and pattern of radiographic hand osteoarthritis and association with pain and disability (the Rotterdam study). *Annals of the Rheumatic Diseases*. 2005;64(5):682-687. doi:10.1136/ard.2004.023564

13. Wallace G, Cro S, Doré C, et al. Associations Between Clinical Evidence of Inflammation and Synovitis in Symptomatic Knee Osteoarthritis: A Cross-Sectional Substudy. *Arthritis Care Res (Hoboken)*. 2017;69(9):1340-1348. doi:10.1002/acr.23162

14. Torres L, Dunlop DD, Peterfy C, et al. The relationship between specific tissue lesions and pain severity in persons with knee osteoarthritis. *Osteoarthritis Cartilage*. 2006;14(10):1033-1040. doi:10.1016/j.joca.2006.03.015

15. Hill CL, Gale DG, Chaisson CE, et al. Knee effusions, popliteal cysts, and synovial thickening: association with knee pain in osteoarthritis. *J Rheumatol*. 2001;28(6):1330-1337.

16. Mathiessen A, Conaghan PG. Synovitis in osteoarthritis: current understanding with therapeutic implications. *Arthritis Res Ther*. 2017;19(1):18. doi:10.1186/s13075-017-1229-9

17. Roemer FW, Guermazi A, Felson DT, et al. Presence of MRI-detected joint effusion and synovitis increases the risk of cartilage loss in knees without osteoarthritis at 30-month follow-up: the MOST study. *Ann Rheum Dis*. 2011;70(10):1804. doi:10.1136/ard.2011.150243

18. Bruyn GA, Naredo E, Damjanov N, et al. An OMERACT reliability exercise of inflammatory and structural abnormalities in patients with knee osteoarthritis using ultrasound assessment. *Ann Rheum Dis*. 2016;75(5):842-846. doi:10.1136/annrheumdis-2014-206774

19. Hall M, Doherty S, Courtney P, Latief K, Zhang W, Doherty M. Synovial pathology detected on ultrasound correlates with the severity of radiographic knee osteoarthritis more than with symptoms. *Osteoarthritis Cartilage*. 2014;22(10):1627-1633. doi:10.1016/j.joca.2014.05.025

20. Naredo E, Cabero F, Palop MJ, Collado P, Cruz A, Crespo M. Ultrasonographic findings in knee osteoarthritis: A comparative study with clinical and radiographic assessment. *Osteoarthritis and Cartilage*. 2005;13(7):568-574. doi:10.1016/j.joca.2005.02.008

21. D'Agostino MA, Terslev L, Aegerter P, et al. Scoring ultrasound synovitis in rheumatoid arthritis: a EULAR-OMERACT ultrasound taskforce — Part 1: definition and development of a standardised, consensus-based scoring system. *RMD Open*. 2017;3(1):e000428. doi:10.1136/rmdopen-2016-000428

22. Terslev L, Naredo E, Aegerter P, et al. Scoring ultrasound synovitis in rheumatoid arthritis: a EULAR-OMERACT ultrasound taskforce-Part 2: reliability and application to multiple joints of a standardised consensus-based scoring system. *RMD Open*. 2017;3(1):e000427. doi:10.1136/rmdopen-2016-000427

23. Barron OA, Eaton RG. Save the trapezium: Double interposition arthroplasty for the treatment of stage IV disease of the basal joint. *The Journal of Hand Surgery*. 1998;23(2):196-204. doi:10.1016/S0363-5023(98)80114-7

24. Eaton RG, Glickel SZ. Trapeziometacarpal osteoarthritis. Staging as a rationale for treatment. *Hand Clin*.
1987;3(4):455-471.

25. Benito MJ. Synovial tissue inflammation in early and late osteoarthritis. *Annals of the Rheumatic Diseases*. 2005;64(9):1263-1267. doi:10.1136/ard.2004.025270

26. D. Smith M. The Normal Synovium. *TORJ*. 2011;5(1):100-106. doi:10.2174/1874312901105010100

27. Wenham CYJ, Conaghan PG. The role of synovitis in osteoarthritis. *Therapeutic Advances in Musculoskeletal*. 2010;2(6):349-359. doi:10.1177/1759720X10378373

28. Ene R, Sinescu RD, Ene P, Cîrstoiu MM, Cîrstoiu FC. Synovial inflammation in patients with different stages of knee osteoarthritis. *Rom J Morphol Embryol*. 2015;56(1):169-173.

Chapter 4

4 Conclusions and Future Directions

This chapter summarizes the original aims of this thesis and the findings from Chapters 2 and 3. Additionally, Chapter 4 will explore the limitations associated with this work, present potential solutions, and recommend directions for future research.

4.1 Overview and Research Objectives

CMC1 OA is one of the most common forms of osteoarthritis observed in the hands and wrist, leading to debilitating pain, functional disability, and decreased quality of life[1]. Radiography and MRI are the current gold standards for diagnosing and monitoring CMC1 OA progression. However, studies have reported significant discrepancies between radiographic evidence of OA and patient-reported outcomes such as pain and disability[2-5]. This discordance has been attributed to the lack of soft-tissue contrast associated with x-ray imaging, limiting its ability to visualize synovial effusion and hypertrophy. MRI is an excellent tool for visualizing synovial tissue but is not feasible for frequent long-term monitoring of CMC1 OA due to its high operating costs and limited accessibility. While conventional 2D US is an attractive alternative to overcome the limitations of MRI and x-ray imaging, it is associated with several limitations. Firstly, operators are required to mentally transform a series of 2D US images into the required 3D anatomy, increasing variability. Secondly, synovial tissue volume measurements acquired using 2D US are highly variable and dependent on operator skill. 3D US imaging techniques present a novel method for overcoming the limitations associated with the previously mentioned imaging modalities. 3D US techniques

include translating the US transducer while continuously acquiring images that are then reconstructed by software to form 3D images of the anatomy[6].

The purpose of this work was to evaluate the use of a novel 3D US imaging device for measuring synovial tissue volumes and investigate the relationship between synovitis phenotypes and pain in patients with CMC1 OA. The central hypothesis of this thesis was that 3D US would be able to quantify synovial tissue volumes as accurately and precisely as the current gold standard of MRI. Additionally, we hypothesized that these 3D US acquired volumes would potentially be a new imaging biomarker for the progression of CMC 1 OA.

4.2 Summary

In Chapter 2, we aimed to demonstrate the validity and reliability of our 3D US imaging device for measuring synovial tissue volumes in the CMC1 joint and compared these quantifications against MRI. The linear and volumetric measurement capabilities of the 3D US device were tested on various imaging phantoms and in a CMC1 OA patient population. The results of Chapter 2 indicate that 3D US and MRI are associated with strong concurrent validity and reliability when measuring synovial tissue volume in the CMC1 joint. Our rater-reliability results show that multiple trained raters can make segmentations over multiple trials while still providing excellent reliability (ICC>0.9). 3D US has been proven to be precise and accurate when measuring synovial tissue volumes in the CMC1 joint. We believe that it can be used to provide clinicians with visual features depicting what is happening pathologically in the joint. As the performance capabilities of the described 3D US device have been tested in a musculoskeletal population, the next step was to examine the sonographic features associated with these 3D US images. Using these images, we assessed what information could be observed and how it could potentially be useful for clinical practice and health research.

In Chapter 3, the aim was to apply the validation findings of 3D US in a CMC1 patient population to better understand how synovial tissue volume relates to patient-reported outcomes such as pain, stiffness and disability. The second goal of this chapter was to describe the different synovitis phenotypes observed in US within this population to evaluate how different morphology may influence patient outcomes. 3D US, 2D US, and plain x-ray radiographic images of 19 CMC1 OA patients were acquired. Additionally, these patients were asked to complete an AUSCAN survey and a pinch grip test. To test the relationship between the various imaging grading systems and patient-outcomes, a stepwise linear regression was conducted.

The second study (Chapter 3) demonstrated three distinct morphological presentations of synovitis. These consisted of synovial effusion dominant features, diffuse effusion and increased hypertrophic features, and osteochondral dominant features. These phenotypes were distinguished by synovial tissue margin properties, synovial tissue volume, and histological features of synovitis (effusion vs. hypertrophy). The trends observed in this pilot study may follow histological trends described in multiple OA studies, where synovitis is a dominant feature in earlier stages of OA, but osteochondral involvement increases as the disease progresses [7-10]. The use of sonographic features in clinical practice is important as it could provide additional information on OA pathology and patient-specific factors such as predisposition, pathological mechanisms, and treatment response. Identifying sonographic phenotypes is important as many pathological features associated with early OA could be missed with our current methods of imaging OA patients in the clinic (x-rays). There is still much we do not know about the initial stages of OA development. Patients may vary in that their OA progression and symptoms may be mechanically or inflammatory driven and as such,

would require different imaging analysis and treatment approaches. A combination of x-ray and US imaging may provide the base for a composite scoring that could identify the underlying mechanisms of disease progression for each patient and provide better direction for clinical trials and treatment programs in the future. 3D US is a rapid and easy method for monitoring changes in joint and soft tissue structure which may be better suited for acquiring images on OA over long periods of time, as is the case with longitudinal monitoring. 3D US has the potential to improve clinical and research workflow while quantitatively describing synovial tissue volumes in CMC1 OA patients; however we suggest that more work is required to investigate how sonographic features of CMC1 OA are useful in OA research and in a clinical setting.

4.3 Limitations

It is important to note that there were several limitations associated with this work. Firstly, the CMC1 OA patient who participated in this study were recruited by a hand surgeon indicating that they are at a stage in OA progression where surgical intervention is an option. The majority of patients in this study had stage 3 radiographic evidence of OA based on the EL scale. Thus, we were missing information about individuals who are in the early stages of OA development and therefore cannot make conclusions on how accurate 3D US would be when distinguishing between healthy individuals and those with early OA. Additionally, as we are only seeing patients who have consulted clinicians about their thumb pain, we are potentially missing those patients who may be showing signs of OA but have not deemed it necessary to consult a physician. Future research studies should consider recruiting patients from primary care or rheumatology clinics as there may be a larger variation in patients.

Secondly, although we were able to control for the effects of intra-articular corticosteroid injections by waiting for the activation period of the drugs to pass, we were not able to control for the administration of non-prescription pain medication. This could potentially have influenced patient-reported outcomes such as pain and physical dysfunction. Additionally, the AUSCAN survey is intended for the measurement of global hand pain and is not specifically designed for the CMC1 joint. This influenced patient's answers on the survey as many of the items did not relate to actions that would elicit pain in the CMC1 joint. However, at the time of this study, the AUSCAN was deemed the most appropriate survey for evaluating pain,stiffness and disability in CMC 1 OA patients.

Thirdly, since this work followed a cross-sectional study design, we were not able to observe how changes in synovial tissue volume and morphology impact patient outcomes over time. A longitudinal study design could potentially provide information about how the joint changes long term and whether features such as flare-ups have a significant impact on metrics of synovial tissue volume, AUSCAN score, grip strength, and imaging grading. Finally, the acquired images in this work were only of the volar side of the joint as imaging through the thenar eminence provided superior visualization of the joint. However, synovitis is not always isolated to one area of the joint, and unfortunately, due to the nature of ultrasound and its inability to penetrate bone, we are missing information about the amount of inflammation inside the joint. We are also missing information about the dorsal side of the joint where synovitis can also be observed in some patients. In light of these limitations, more work is needed before the clinical implementation of 3D US for CMC1 OA can be considered.

4.4 Future Directions

The results of these studies highlight the potential for 3D US for quantitatively characterizing synovitis and assessing CMC1 OA disease status, progression, and treatment. In Chapter 3, we discussed the morphological features of the CMC1 OA joint in US and compared synovial tissue volume to measures of pain. This study was cross-sectional, but we believe that a longitudinal study would be better suited to investigate how synovitis changes over time and how these changes correlate to patient-reported outcomes. We also believe that the inclusion of histology with 3D US imaging studies would be a valuable method for confirming the changes we are observing in the tissues as the disease progresses.

Future studies will investigate methods for combining multiple 3D US images to increase the field of view and potentially view all angles of the CMC1 joint. This would allow for more complete visualization of the joint, which would give clinicians an accurate assessment of synovial tissue volume. Additionally, to address concerns about manual segmentation variability and efficiency, future studies aim to integrate deep learning algorithms into our 3D US system. The efficacy of convoluted neural networks has been assessed in MRI for lesion detection and segmentation creation and has shown promising results[11,12].

4.5 Conclusion

In conclusion, this thesis investigates the development and application of a mechanical 3D US imaging device for monitoring synovitis in CMC1 OA patients. The studies described in this thesis demonstrate that 3D US is able to be used for measuring synovial tissue volume with strong concurrent validity with MRI and with excellent rater reliability. Furthermore, 3D

US is an alternative imaging method, which has the ability to provide volumetric visualization of the desired region without the need for costly equipment or a time-consuming procedure.

4.6 References

1. Dandy DJ. *Essential Orthopaedics and Trauma*. 2nd ed. Churchill Livingstone; 1993.

2. Hannan MT, Felson DT, Pincus T. Analysis of the discordance between radiographic changes and knee pain in osteoarthritis of the knee. *J Rheumatol*. 2000;27(6):1513-1517.

3. Bedson J, Croft PR. The discordance between clinical and radiographic knee osteoarthritis: A systematic search and summary of the literature. *BMC Musculoskelet Disord*. 2008;9(1):116. doi:10.1186/1471-2474-9-116

4. Birrell F, Croft P, Cooper C, Hosie G, Macfarlane G, Silman A. Health impact of pain in the hip region with and without radiographic evidence of osteoarthritis: a study of new attenders to primary care. The PCR Hip Study Group. *Ann Rheum Dis*. 2000;59(11):857-863. doi:10.1136/ard.59.11.857

5. Clancey GJ. Radiograph Assessment of the Basal Thumb Joint: *Orthopaedic Nursing*. 1989;8(4):58-59. doi:10.1097/00006416-198907000-00021

6. Fenster A, Downey DB, Cardinal HN. Three-dimensional ultrasound imaging. *Phys Med Biol*. 2001;46(5):R67-R99. doi:https://doi.org/10.1088/0031-9155/46/ 5/201.

7. D. Smith M. The Normal Synovium. *TORJ*. 2011;5(1):100-106. doi:10.2174/1874312901105010100

8. Benito MJ. Synovial tissue inflammation in early and late osteoarthritis. *Annals of the Rheumatic Diseases*. 2005;64(9):1263-1267. doi:10.1136/ard.2004.025270

9. Wenham CYJ, Conaghan PG. The role of synovitis in osteoarthritis. *Therapeutic Advances in Musculoskeletal*. 2010;2(6):349-359. doi:10.1177/1759720X10378373

10. Ene R, Sinescu RD, Ene P, Cîrstoiu MM, Cîrstoiu FC. Synovial inflammation in patients with different stages of knee osteoarthritis. *Rom J Morphol Embryol*. 2015;56(1):169-173.

11. Chea P, Mandell JC. Current applications and future directions of deep learning in musculoskeletal radiology. *Skeletal Radiol*. 2020;49(2):183-197. doi:10.1007/s00256-019-03284-z

12. Schwartz AJ, Clarke HD, Spangehl MJ, Bingham JS, Etzioni DA, Neville MR. Can a Convolutional Neural Network Classify Knee Osteoarthritis on Plain Radiographs as Accurately as Fellowship-Trained Knee Arthroplasty Surgeons? *The Journal of Arthroplasty*. 2020;35(9):2423-2428. doi:10.1016/j.arth.2020.04.059

Appendices

Appendix A: Research ethics board approval letter

Date: 23 April 2021

To: Dr. Emily Lalone

Project ID: 118016

Study Title: Can Unresolved Inflammation Lead to Poor Patient Outcomes Following Fracture?
-Integrating Mechanics and Biology of Chronic Inflammation to Improve Wrist Fracture Outcomes

Application Type: HSREB Initial Application

Review Type: Delegated

Full Board Reporting Date: 06/Apr/2021 13:00

Date Approval Issued: 23/Apr/2021 07:02

REB Approval Expiry Date: 23/Apr/2022

Dear Dr. Emily Lalone

The Western University Health Science Research Ethics Board (HSREB) has reviewed and approved the above mentioned study as described in the WREM application form, as of the HSREB Initial Approval Date noted above. This research study is to be conducted by the investigator noted above. **All other required institutional approvals and mandated training must also be obtained prior to the conduct of the study**.

Documents Approved:

Document Name	Document Type	Document Date	Document Version
Data_collection_form_Nov-19-2020-v1.0	Other Data Collection Instruments	19/Nov/2020	1.0
InvitationPoster-Apr-09-2021-v1.2	Recruitment Materials	09/Apr/2021	1.2
3DUS Wrist -Study Protocol-Apr_21_2021_V1.4	Protocol	21/Apr/2021	1.4
LOI-1CMC-Apr-21-2021-v1.3	Written Consent/Assent	21/Apr/2021	1.3
LOI-DRF-Apr-21-2021-v1.3	Written Consent/Assent	21/Apr/2021	1.3
LOI-Healthy-Apr-21-2021-v1.3	Written Consent/Assent	21/Apr/2021	1.3

Documents Acknowledged:

Document Name	Document Type	Document Date	Document Version
WSS CIHR Success Seed-Budget	Study budget		

No deviations from, or changes to, the protocol or WREM application should be initiated without prior written approval of an appropriate amendment from Western HSREB , except when necessary to eliminate immediate hazard(s) to study participants or when the change(s) involves only administrative or logistical aspects of the trial.

REB members involved in the research project do not participate in the review, discussion or decision.

The Western University HSREB operates in compliance with, and is constituted in accordance with, the requirements of the TriCouncil Policy Statement: Ethical Conduct for Research Involving Humans (TCPS 2); the International Conference on Harmonisation Good Clinical Practice Consolidated Guideline (ICH GCP); Part C, Division 5 of the Food and Drug Regulations; Part 4 of the Natural Health Products Regulations; Part 3 of the Medical Devices Regulations and the provisions of the Ontario Personal Health Information Protection Act (PHIPA 2004) and its applicable regulations. The HSREB is registered with the U.S. Department of Health & Human Services under the IRB registration number IRB 00000940.

Please do not hesitate to contact us if you have any questions.

Sincerely,

Ms. Nicola Geoghegan-Morphet , Ethics Officer on behalf of Dr. Philip Jones, HSREB Chair

Note: This correspondence includes an electronic signature (validation and approval via an online system that is compliant with all regulations).

CURRICULUM VITAE

Education & Training

2020 – Current

Masters of Science (MSc) in Kinesiology Integrative Biosciences
University of Western Ontario, London, ON
Supervisors: Dr. Emily Lalone, Dr. Aaron Fenster
Thesis: "Three-dimensional Ultrasound Imaging for Characterization of Synovitis in First Carpometacarpal Osteoarthritis"

2016 – 2016

Bachelor of Arts (BA) Honours Double Major
Majors: Kinesiology and Rehabilitation Sciences
University of Western Ontario, London, ON

2021

Indigenous Canada Certification
University of Alberta, Edmonton, AB

2020 - 2021

Canadian Rheumatology Ultrasound Basic Certification
Canadian Rheumatology Ultrasound Society
Toronto, ON

2019-2020

Emergency First Responder Certification
Canadian Red Cross, Toronto, ON

Awards

2021-2022

Transdisciplinary Bone and Joint Training Award
Western University Bone and Joint Institute

2017 – 2019

Academic All Canadian Award - U-Sport
U-Sport Canada
Awarded to exceptional student-athletes who achieve an academic standing of 80% or better while playing on their university's varsity team.
National

2017 – 2020

Dean's Honour List
Faculty of Health Sciences & Department of Kinesiology, Western University, Canada
Full-time students who completed a minimum of 4.0 courses during the previous fall/winter session and earned an average of 80% or more with no failed courses
Institutional

2016

Duke of Edinburgh's International Gold Award
Awarded for helping the community/environment, becoming fitter, developing new skills, planning, training for and completing an expedition and, for Gold only, working with a team on a residential activity.
International

2016

The Western Scholarship of Excellence
Western University, London, ON, Canada
Awarded to the student with the top high school admission average entering an undergraduate degree.
Institutional

Research Experience

2020 – Current

Robarts Research Institute
School of Kinesiology, Western University, Canada, London, ON
Supervisors: Dr. Emily Lalone, Dr, Aaron Fenster
Projects:

1. Validating the measurement characteristics of a new 3D ultrasound device for the hands and wrists
2. Three-dimensional ultrasound to investigate effusion synovitis in the hand and wrist of osteoarthritis patients
3. Automatic knee cartilage segmentation using deep learning on healthy 3D knee images.
4. Spatially tracked whole-breast three-dimensional ultrasound system toward point-of-care breast cancer screening in high-risk women with dense breasts.

2019-2020

Robarts Research Institute
School of Kinesiology, Western University, Canada, London, ON
Supervisors: Dr. Arthur Brown
Projects: Investigating the activity of GSK3B in a mouse model of concussion over time.

Teaching Experience

Fall 2020

Graduate Teaching Assistant
Course: Athletic Injuries (Kinesiology 2236)
Supervisor: Dave Humphreys

Winter 2021

Graduate Teaching Assistant
Course: Biomechanics (Kinesiology 3353)
Supervisor: Dr. Derek Pamukoff

Fall 2021-Winter 2022

Graduate Teaching Assistant
Course: Athletic Injuries (Kinesiology 3336)
Supervisor: Dave Humphreys

Committee & Team Participation

2019-2020	**Vice President & Advocacy Department Head, Autism Awareness Western** Western University, London, ON, Canada
2016-2019	**Team Member, Women's Varsity Rugby** Western University, London, ON, Canada
2016-2019	**General Member, Western University Mustangs Care** Western University, London, ON, Canada
2016-2019	**General Member, Autism Awareness Western** Western University, London, ON, Canada
2017-2018	**General Member, Health Occupations Students of America** Western University, London, ON, Canada

Professional Membership

2020 – 2022	**Canadian Rheumatology Ultrasound Society (CRUS)** Toronto, Canada Student member
2020 – 2022	**Orthopedic Research Society** Rosemont, Illinois, USA Student member
2020 – 2022	**Osteoarthritis Research Society International** Liverpool, UK Student member
2020 – 2022	**Ontario Kinesiology Association** Toronto, Canada Student member

Publications & Presentations

Peer- Reviewed Journal Manuscripts (1)

1. Claire Park et al. "Spatially tracked whole-breast three-dimensional ultrasound system toward point-of-care breast cancer screening in high-risk women with dense breasts". *Medical physics (Lancaster)*. 23 March 2022. Published online 2022. doi:10.1002/mp.15632

Peer- Reviewed Conference Abstracts (1)

1. **Carla du Toit**, Robert Dima, Nina Suh, Aaron Fenster, Emily Lalone, "3D ultrasound for diagnosis and tracking of synovitis in first carpometacarpal osteoarthritis patients," Proc. SPIE 12038, Medical Imaging 2022: Ultrasonic Imaging and Tomography, 120380I (4 April 2022);https://doi-org.proxy1.lib.uwo.ca/10.1117/12.2613001
2.

Oral Presentations (5)

1. **C. Du Toit,** D. Tessier, A. Fenster, E. Lalone, "3D Ultrasound to Investigate Effusion Synovitis in the Hand and Wrist" *Imaging Network Ontario 2021 Symposium*. 23-24 March 2021. (Provincial; Virtual)

2. **C. Du Toit,** D. Tessier, A. Fenster, E. Lalone, "Three-dimensional Ultrasound to Investigate Effusion Synovitis in the Hand and Wrist" *Western University Kinesiology Gradual Research Day*. 22 February 2021. (Regional; Virtual)

3. **C.du Toit**, R.Dima, A. Fenster, E. Lalone, " 3D Ultrasound Techniques for Evaluation of Synovitis in Patients with Osteoarthritis" *SonoCan2021.* 3 October 2021. (National; Virtual)

4. **C. Du Toit,** R.Dima, S. Papernick**,** D. Tessier, A. Fenster, E. Lalone, "3D Ultrasound to Characterize Synovial Tissue Volume in First Carpometacarpal Osteoarthritis Patients" *Imaging Network Ontario 2021 Symposium*. 23-24 March 2022. (Provincial; Virtual)

5. C du Toit, R. Dima, S.Papernick, D.Tessier, A. Fenster, E. Lalone,"3D Ultrasound for Diagnosis and Tracking of Synovitis in First Carpometacarpal Osteoarthritis Patients" Society of Photographic Instrumentation Engineers (SPIE) Medical Imaging: Ultrasonic Imaging and Tomography. 23 February 2022. (International; In Person)

Poster Presentations (4)

1. **C. Du Toit,** D. Tessier, A. Fenster, E. Lalone, "3D Ultrasound to Investigate Synovitis in the Hand and Wrist". Osteoarthritis Research Society International 2021(OARSI). 29 April – 1 May 2021. (International; Virtual)

2. **C. Du Toit,** D. Tessier, A. Fenster, E. Lalone, "Three-Dimensional Ultrasound to Investigate Synovitis in the Hand and Wrist". Robarts Research Retreat, Western University. 17-18 June 2021. (Regional; Virtual)

3. **C. Du Toit**, R.Dima**,** S. Papernick**,** D. Tessier, A. Fenster, E. Lalone, "Three-Dimensional Ultrasound for Assesment of Synovitis in Carpometacarpal Osteoarthritis Patients". Osteoarthritis Research Society International 2022 (OARSI). 4 April 2022. (International; Virtual)

4. **C. Du Toit**, R.Dima**,** S. Papernick**,** D. Tessier, A. Fenster, E. Lalone "3D Ultrasound for Monitoring Synovitis in First Carpometacarpal Osteoarthritis Patients. Orthopaedic Research Society 2022. 4 February 2022. (International; In Person)

Professional & Volunteering Activities

Volunteering:

2019 – 2020	**Cross- Country Student Athletic Trainer** *Supervisor:* Dave Humphreys & Guy Schultz University of Western Ontario | London, ON
Summer 2019	**Physiotherapy Volunteer** *Supervisor:* Troy Harvie Windsor Physiotherapy, Windsor, NS
2019 -2020	**Physiotherapy Volunteer** *Supervisor:* Chris Statten Reactive Physiotherapy, London, ON
2016 – 2019	**Mustangs Care** University of Western Ontario, London, ON
2016-2019	**Western Women's Rugby Highschool Skills Workshops** University of Western Ontario, London, ON
Summer 2018	**Physiotherapy Volunteer** *Supervisor:* Marelise Wilson Tri Physio, Bloemfontein, SA

Professional:

Summer 2018 Spring/Summer 2020	**Therapeutic Recreation Therapist** Riverview Enhanced Living Centre
2014 - 2020	**Assistant Medical Secretary** Medical Arts Center, Bridgewater, NS
2021	**Data Specialist** Big Data Science, Stratford, ON